NPL

NPL REPORT AS 68

Final Report on the Physico-Chemical Characterisation of PROSPEcT Engineered Nanomaterials

Ratna Tantra, Robert Boyd, Alex Cackett, Tony Fry, Dipak Gohil, Sophia Goldberg, Joanna Lee, Caterina Minelli, Roger Peck, Paul Quincey, Steve Smith, Jackie Snowden, Steve Spencer, Jordan Tompkins, Jian Wang and Li Yang.

FEBRUARY 2012

Final Report on the Physico-Chemical Characterisation of PROSPEcT Engineered Nanomaterials

Ratna Tantra, Robert Boyd, Alex Cackett, Tony Fry, Dipak Gohil, Sophia Goldberg, Joanna Lee, Caterina Minelli, Roger Peck, Paul Quincey, Steve Smith, Jackie Snowden, Steve Spencer, Jordan Tompkins, Jian Wang and Li Yang.

Analytical Science and Material Divisions, NPL

ISSN: 1754-2928

National Physical Laboratory
Hampton Road, Teddington, Middlesex, TW11 0LW

Approved on behalf of NPLML by Alex Shard, Divisional Knowledge Leader

CONTENTS

ABSTRACT

The PROSPEcT project represents the UK's contribution to an OECD WPMN (Organisation for Economic Co-operation and Development, Working Party on Manufactured Nanomaterials) sponsorship programme. The National Physical Laboratory (NPL) core activity relates to the physicochemical testing of manufactured CeO_2 and ZnO nanomaterials. This is in support of the ecotoxicological investigations to study their potential risk in the damage of the aquatic environment, which will be commented on in Chapter 1. The output of the core activity is reported in the main body of the report (Chapter 2), which consists of a summary of test results of the nanopowders: *as received*, when dispersed in one of four ecotox liquid media and when aerosolised. For the purposes of synchronisation and harmonisation, this data is also reported in the NAPIRA hub (www.nanohub.eu), a central European database. In acquiring the core data, trends were observed between the measured particle size and other parameters, such as: specific surface area, dispersion stability and dissolution kinetics. The ability to make such correlations is important as this means that the number of physicochemical parameters required for testing can be reduced in the future. However, without further evidence (namely, correlation with other data generated within the consortium and the ability to analyse the large amount of data objectively) it is difficult, at this stage, to deduce the most relevant physicochemical properties to complement the toxicity assessment.

In addition to the core activity, NPL was also involved in tackling various measurement issues (as detailed in the appendices) in:

a) understanding potential sources of variability in measurements, which can come: by not following a standard protocol and/or treating the measurement tool as a black box (thus not understanding their inherent limitations).
b) conducting homogeneity testing of samples (as organised by the Joint Research Centre (JRC), in which samples received have been subsampled first by Whitehouse Scientific and further subsampled by JRC. For the full history of the powders, please refer to Section 2.1.1. NPL's role was for the provision of data towards the assessment of the homogeneity of the subsamples, for potential reference material development.
c) developing appropriate new technologies, which is necessary to improve future data reliability. New technological platforms under investigation to include: the use of an ozone based cleaning unit in order to remove background such as carbaceous contamination (to improve selectivity), Time of Flight Secondary Ion Mass Spectrometry (TOF-SIMS) as a potential tool to measure surface chemistry (and subsequently perform depth profiles of adsorbents on the surface of nanomaterials), development of charge particle counting technology, protocols for the characterisation of the photocatalytic properties of nanomaterials and a microfluidic based technique for potential high throughput screening methods for the determination of dissolution. The ozone based cleaning unit involved the building and testing of a prototype, which was shown to be *not fit for purpose.* The latter four technologies showed potential for nanomaterial characterisation and are at further developmental stage.

Lastly, we have identified the knowledge gaps, which include the:

a) need for better measurement tools
b) lack of suitable reference materials for testing
c) lack of experimental investigations that will have a direct impact on risk assessment.

If such issues are not dealt with, then questions surrounding nanotoxicity will forever remain inconclusive.

CHAPTER 1 INTRODUCTION

To determine the safety of nanomaterials, the nano(eco)tox community is concentrating on two research activities:

a) Physicochemical characterisation.
b) Toxicity testing, either *in vivo* or *in vitro*.

Both are needed in order to understand the biological action, fate, behaviour and exposure of nanomaterials. Realistic risk assessment requires the use of statistically meaningful data (through the use of standards/standardisation and reference materials) and well-validated models for their interpretation, both of which highlight the strong need for metrology (Figure 1). Although the role of metrology in nano(eco)toxicological field is currently relatively small and poorly understood, it is vital. In the past, the lack of standardised methods and reference materials has been blamed for irreproducible and inconclusive findings.

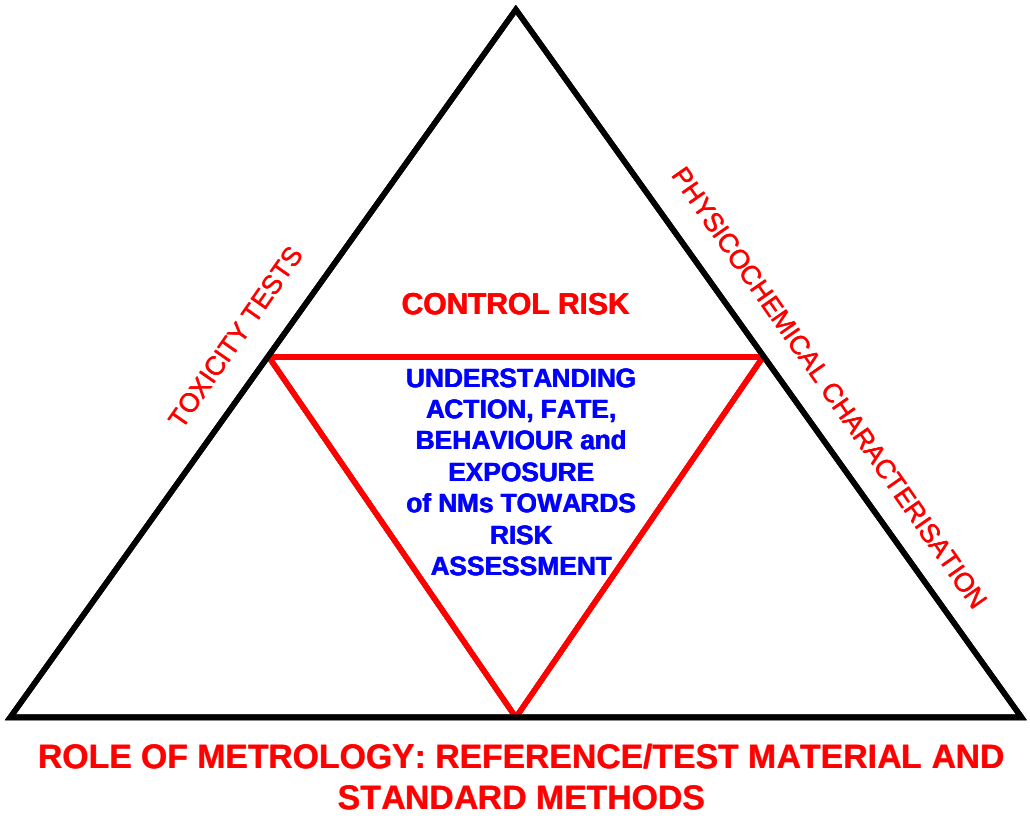

Figure 1. Current Nanomaterial Research Strategy to understand, predict and control the health and environmental risks associated with nanomaterials.

NPL is contributing to the PROSPEcT project on nano-safety by:

a) Provision of physicochemical core data, good research protocols (as achieved through extensive literature research and the inclusion of guidelines provided by relevant/existing standard documents). These protocols were applied in the testing of PROSPEcT ZnO and CeO_2 powders ("as-received" powders, dispersion in appropriate liquid media and aerosolised) using suitable techniques. Steps prior to characterisation are considered to be critical and the protocols surrounding powder handling, subsampling and dispersion are described. Details of the core parameters investigated and the analysis protocols using the various techniques employed in this investigation are summarised in Table 26 and Table 27, in Appendix 3.

b) Undertaking metrology based research, to include:
    1) conducting studies, aimed at understanding the strengths and limitations of the various techniques employed, and how the lack of standardised protocols could contribute to errors in the interpretation of the data.
    2) the development of new techniques for better characterisation, which included: the development of new aerosol technology to discriminate background particles from engineered nanomaterials, improved surface chemistry/depth profiling measurements of adsorbed species and microfluidics 'lab on chip' technology for high-throughput measurement of dissolution kinetics.
    3) conducting homogeneity tests; our participation here is as a testing laboratory in this JRC-led initiative, for the assessment of the PROSPEcT powders as potential reference materials.

The output of our core PROSPEcT activity is detailed in Chapter 2 of this report. Appendix 2 reflects on the various studies conducted in addition to the core activity (although still within the scope of PROSPEcT). The description associated with these additional studies is not within scope of this report and for further details, the reader is referred to other published reports/documents. It is the core activity of PROSPEcT (Figure 2) i.e. the final provision of technical dossiers (through NIA) that is of upmost importance and will contribute towards data required to better regulate these materials. Figure 2 below shows that there is a need to improve regulation, as the current threshold limit of one tonne per year for nanomaterial registration (with ECHA) is the same as that for chemicals. There are clear differences between particles and chemicals and this threshold limit may change in the future as a consequence of this. But this will be dependent on regulatory associated bodies such as: REACH (Registration, Evaluation, Authorisation & restriction of CHemicals), SCENIRH (Scientific Committee on Emerging and Newly Identified Health Risks) and ETUC (European Trade Union Confederation).

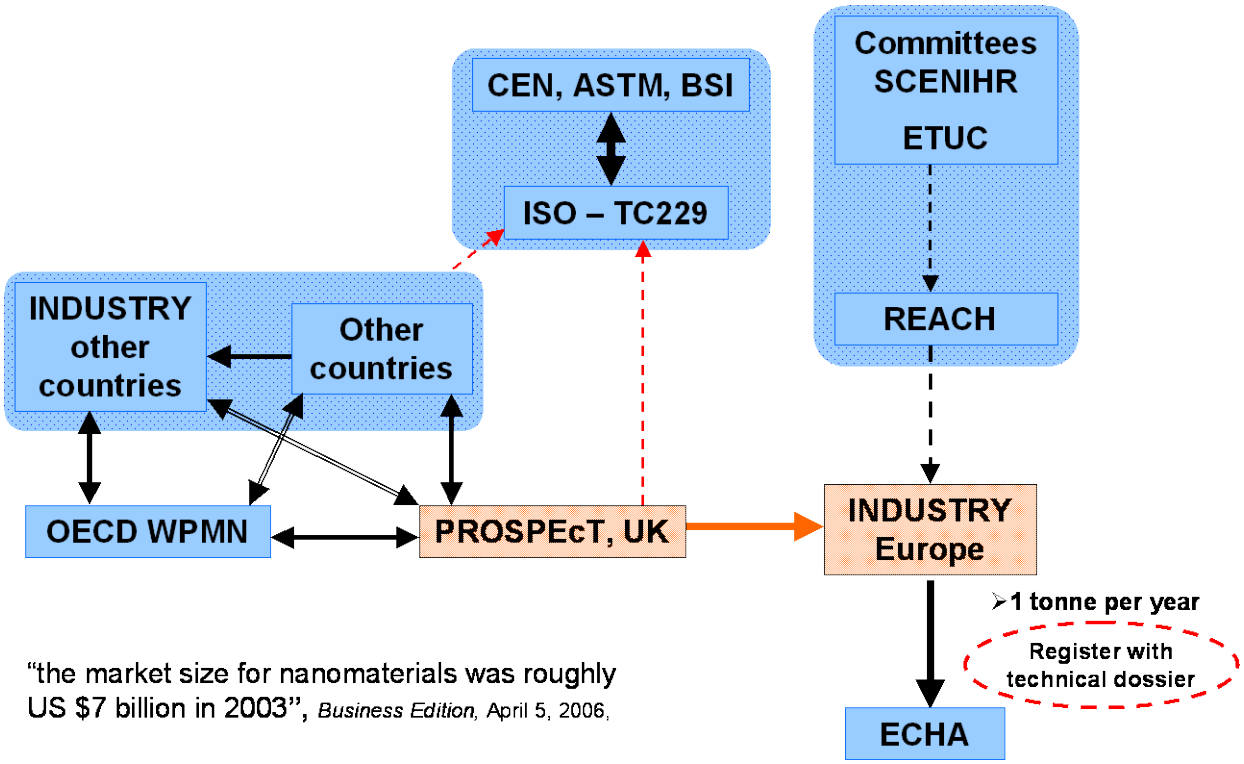

Figure 2. An overview of PROSPEcT in the context of Global Nanomaterials Safety Initiatives

Although the PROSPEcT consortium mainly comprises of UK partners, the project is well linked globally. In an attempt to improve PROSPEcT participation in standardisation, the outputs from this project have been linked with activity under ISO – ISO/TC 229 - Nanotechnologies - committee dedicated to the standardisation in the field of nanotechnologies; this committee is currently chaired by the UK with strong participation by Drs Charles Clifford and Mark Gee (NPL personnel). ISO has co-operation from other stakeholders in the area including CEN (The European Committee for Standardization), BSI (British Standards Institutions) and ASTM (American Society for Testing and Materials).

CHAPTER 2 OECD CORE ACTIVITY

2.1 METHODS AND INSTRUMENTATION

2.1.1 Materials

Nanomaterials supplied from the PROSPEcT programme are summarised below in Table 1.

Table 1. Sample name and supplier of PROSPEcT powders.

Given Sample Name	Supplier
A. Nanograin CeO_2	Umicore Belgium
B. Nanosun ZnO	Micronisers, Australia
C. Z-COTE HP 1 ZnO	BASF, Germany
D. Micron ZnO	Sigma Aldrich, UK
E. Z-COTE ZnO	BASF, Germany
F. Micron CeO_2	Sigma Aldrich, UK
G. Ceria dry CeO_2	Antaria, Australia

Powder History:

The powders were provided by the suppliers and sent to NPL, who received between 10 kg – 20 kg of each type of nanomaterial. This material was sent out to Whitehouse Scientific Ltd to be spin riffled into smaller amounts (~ 250g placed in pre-cleaned amber coloured 1 L glass bottles (Qorpak)). The decision to use spin riffling as the first stage of the subsampling process was made due to practical reasons when subsampling tens of kg worth of material into manageable volumes. Each bottle was designated an associated batch number. The riffled powders were sent to other partners in the consortium. At NPL, the powders were further subsampled by scooping the powder out from the glass bottles into smaller 60 ml pre-cleaned amber coloured glass pots (Qorpak) and were given the same batch number as their corresponding 1 L bottles, immediately followed by forward slash ("/"), then a letter/word or character to signify the further subsampling from the 1 L bottles. For analysis using various techniques (depending on the quantity required), additional subsampling was performed by further scooping sampling of the material.

Half way through the project, some of the 1 L bottles were transferred to JRC for subsequent riffling of into 0.5 – 2 g quantities. For consistency, NPL decided to finish the characterisation using the subsampled 60 ml glass bottles at this stage and only characterised the JRC spin riffled samples for the purpose of establishing quality assurance for homogeneity and for the aerosol characterisation.

Dispersion of nanomaterials in ecotoxicological relevant media (fish medium, daphnia medium and seawater) was carried out in accordance to a previously described protocol (1). In order to ensure consistency across the project, the recipes (chemical compositions) used for making up the ecotox media were obtained from the University of Exeter and details on the media preparation will not be covered here. Deionised (DI) water was used to prepare all aqueous solutions and suspensions. De-ionised water (and in some cases de-ionised water with 5 mM sodium chloride (Sigma Aldrich, UK)) was used as the corresponding *control* media. The NaCl used here served as a background electrolyte for the measurement of zeta-potential. Unless otherwise stated, dispersions of 50 mg /L concentration were made.

The protocols employed for the various instruments used during the acquisition of the OECD identified physicochemical endpoints (as detailed in Table 26) are summarised in Table 27, Appendix 3.

2.1.2 Protocols used prior to physicochemical characterisation

PROSPEcT has identified a set of common protocols prior to characterisation, including:

a) Guidelines and protocols for sampling
b) Protocol for nanoparticle dispersion
c) Video demonstrating the dispersion protocol
d) Evaluation and assignment of nanoparticle dispersion/characterisation methodologies, to be developed under PROSPEcT.

The protocols are accessible via the NIA website:
http://www.nanotechia-prospect.org/publications/basic

2.1.3 Protocols: physicochemical characterisation

The various instruments and protocols employed for nanomaterial characterisation of the PROSPEcT powders ("as received", when dispersed in liquid media and when aerosolised) are summarised in Table 28, Appendix 3.

2.2 RESULTS

2.2.1 Characterisation of the "as received" powders

Electron Microscopy

Electron microscopy provides high resolution images of the nanoparticles from which the mean particle size and size distribution can be determined via the measurement of the individual particles. The "as received" powders were characterised using scanning (SEM) and transmission electron microscopy (TEM) (for details on the sample preparation please see appendix 3). The micrographs were analysed and the corresponding results for SEM and TEM are tabulated in Table 2 and Table 3, respectively. In this report, only the mean primary particle sizes and the corresponding standard deviations (to reflect on the polydispersity of the size distribution) are given; particle size is reported as the Feret diameter. The Feret diameter, also referred to as the calliper diameter, is the distance between two parallel tangents on opposite sides of the particle; here we report on the maximum Feret diameter. The corresponding SEM and TEM images and the particle size distributions (represented in the form of histograms), can be found on the NAPIRA hub database.

Table 2. The size of primary particles, as defined by their corresponding Feret's diameter. Mean diameter (± 1 SD) of a minimum of 50-100 particles measured in the SEM images; the SD here represents the broadness of the size distribution. Data analysis of the images was processed with the use of "transparency sheets method".

Sample Name	Batch number	Mean Feret diameter (nm)
A. Nanograin CeO_2	CB250#41#05	28.4 ± 10.4
B. Nanosun ZnO	ZA250#30#05	42.5 ± 3.6
C. Z-COTE HP 1 ZnO	ZB250#64#05	140.8 ± 65.8
D. Micron ZnO	ZrA250#45#05	891.8 ± 800.0
E. Z-COTE ZnO	ZC250#37#05	151.0 ± 55.6
F. Micron CeO_2	CrA250#40#05	615.3 ± 430.5
G. Ceria dry CeO_2	CA340#13#05	44.9 ± 14.6

Table 3. The size of primary particles, as defined by their corresponding Feret's diameter. Mean diameter (± 1 SD) of a minimum of 200 particles measured in the TEM images; the SD here represents the broadness of the size distribution. Data analysis of the images was processed with the aid of a Tablet PC and a digital pen.

Sample Name	Batch number	Mean Feret diameter (nm)
A. Nanograin CeO_2	CB250#41#ICP	26.9 ± 16.4
B. Nanosun ZnO	ZA250#30#ICP	35.0 ± 12.0
C. Z-COTE HP 1 ZnO	ZB250#64#ICP	69.8 ± 48.5
D. Micron ZnO	ZrA250#33#ICP	143.0 ± 103.4
E. Z-COTE ZnO	ZC250#37#ICP	78.9 ± 50.2
F. Micron CeO_2	CrA250#40#ICP	112.4 ± 74.5
G. Ceria dry CeO_2	CA340#13#ICP	10.2 ± 3.6

From these results, two points become clear. Firstly all of the materials display a high degree of polydispersity apart from the Ceria dry sample (as revealed by TEM imaging). The second is that there is little agreement between the two techniques (apart from the Nanograin CeO_2 and Nanosun ZnO sample), with TEM consistently giving the smaller particle size. For all of the samples analysed by TEM and SEM the primary particles are in the form of agglomerates/aggregates, which means that

particles do not exist as separate, individual entities. TEM has the best overall resolution whilst SEM suffers from an artefact called the edge effect, where surfaces that are not horizontal to the electron beam will appear more intense. If two particles are close together or touching and have edges that slope, this artefact will cause them to appear as a single particle under the SEM.

BET (Brunauer-Emmett-Teller)

This analysis gives a measurement of the area of exposed particle surface (although the measured specific surface area (SSA) may not necessarily mean that which is available) as determined by the adsorption of nitrogen gas. Here, porosity is defined as the volume of pores per gram. The Barrett-Joyner-Halenda (BJH) method was used to determine the porosity. The results are summarised in Table 4 and Table 5.

Table 4. A summary of the specific surface area values for PROSPEcT powders, as obtained by the BET gas adsorption technique. The data is the mean of values (± 2 SD) of two replicates acquired on different days.

Sample Name	Batch number	Mean BET SSA (m^2/g)
A. Nanograin CeO_2	CB250#41#BET1	27.2 ± 0.9
B. Nanosun ZnO	ZA250#30#05	27.2 ± 1.2
C. Z-COTE HP 1 ZnO	ZB250#64#BET1	15.1 ± 0.6
D. Micron ZnO	ZrA250#53#BET1	6.2 ± 0.3
E. Z-COTE ZnO	ZC250#20#BET1	12.4 ± 0.6
F. Micron CeO_2	CrA250#40#BET1	4.30 ± 0.10
G. Ceria dry CeO_2	CA340#13#05	66 ± 2

Table 5. BET porosity results (outsourced to MCA services).

Sample Name	Batch number	Porosity (cm^3/g)
A. Nanograin CeO_2	CB250#41#ICP	0.118098
B. Nanosun ZnO	ZA250#30#ICP	0.158354
C. Z-COTE HP 1 ZnO	ZB250#64#ICP	0.071347
D. Micron ZnO	ZrA250#33#ICP	0.013820
E. Z-COTE ZnO	Zc250#37#ICP	0.041538
F. Micron CeO_2	CrA250#40	0.021829
G. Ceria dry CeO_2	CA340#13#ICP	0.207229

Comparing the SSA (Table 4) results and the particle size measurements by the electron microscopy (TEM (Table 3) and SEM (Table 2)), it can be seen there is a closer agreement between the BET SSA and TEM analysis when compared to SEM. Results show that: a) the sample with the highest surface area is also the one with the smallest particle size b) BET SSA gets smaller with increasing TEM particle size.

By comparing the BET SSA data to the results for BET porosity (Table 5), a positive correlation emerges between the data sets, generally the greater the SSA the greater the sample's porosity.

X-ray Diffraction (XRD)

Traditionally XRD has been used to determine the crystalline structure of materials. However, it can also be used to provide crystallite size by using the Scherrer's equation, which is dependent on the width of the peaks seen in the XRD spectrum. Analysis of the nanomaterial by XRD on the first hand identified that the materials had the expected crystalline structure, with the ZnO being hexagonal (a=3.25 Å, c=5.2 Å) and CeO_2 being cubic (a=5.4 Å). Table 6 shows the crystallite sizes (as calculated using Scherrer's equation) and the corresponding crystalline phases for the PROSPEcT powders.

Table 6. The XRD crystallite size and crystalline phase results of PROSPEcT powders. Crystallite sizes were determined using Scherrer's equation. Further analysis of the XRD traces were sent to Southampton Chemistry Analytical Solutions for the extraction of crystalline phase information.

Sample Name	Batch number	Crystallite Diameter from XRD (nm)	Crystalline Phase from XRD
A. Nanograin CeO_2	CB250#41#05	33.3	Cubic CeO_2
B. Nanosun ZnO	ZA250#30#05	24.1	Hexagonal ZnO
C. Z-COTE HP1 ZnO	ZB250#64#05	33.8	Hexagonal ZnO
D. Micron ZnO	ZrA250#45#05	41.5	Hexagonal ZnO
E. Z-COTE ZnO	ZC250#37#05	41.5	Hexagonal ZnO
F. Micron CeO_2	CrA250#40#05	33.3	Cubic CeO_2
G. Ceria dry CeO_2	CA340#13#05	10.3	Cubic CeO_2

Apart from the Ceria dry and Nanograin CeO_2 samples, there is little relationship between the particle size as measured by TEM and the crystallite diameter from XRD. There are several reasons for this: particles may consist of several crystalline grains and there may be other contributions (such as inhomogeneous strain and instrument effects) affecting the XRD peak width.

X-ray Photoelectron Spectroscopy XPS

XPS is a surface sensitive technique carried out in ultra-high vacuum, which analyses less than the top 10 nm of a sample. It provides quantitative information on the elemental composition (except for hydrogen and helium) with concentrations as low as 0.1 % depending on the element and some chemical state information. The elemental compositions of the different PROSPEcT powders as measured by XPS are summarised in Table 7 below, in which the elemental concentrations of the elements: carbon (C), cerium (Ce), oxygen (O), silicon (Si) and zinc (Zn) are shown.

Table 7. XPS element atomic concentration results of PROSPEcT powders; the powders were made into pellets (see appendix 3) prior to analysis.

Sample Name	Batch number	C 1s (%)	Ce 3d (%)	O 1s (%)	Si 2s (%)	Zn $2p_{3/2}$ (%)
A. Nanograin CeO_2	CB250#41#ICP	33.3	23.8	42.8	0.0	0.0
B. Nanosun ZnO	ZA250#30#ICP	21.4	0.0	40.4	0.0	38.2
C. Z-COTE HP1 ZnO	ZB250#64#ICP	29.8	0.0	37.8	2.1	30.3
D. Micron ZnO	ZrA250#33#ICP	24.0	0.0	39.8	0.0	36.1
E. Z-COTE ZnO	ZC250#37#ICP	22.7	0.0	40.7	0.2	36.3
F. Micron CeO_2	CrA250#40#ICP	35.3	22.0	42.4	0.0	0.2
G. Ceria dry CeO_2	CA340#13#ICP	35.6	22.4	41.9	0.0	0.0

All samples show a significant level of carbon, probably adsorbed from the atmosphere. All values are consistent, except for the Z-COTE HP1 ZnO sample where silicon and more carbon are detected, arising from the silane coating of the nanomaterials. Interestingly, a trace amount of silicon is detected on the Z-COTE ZnO sample. However, the relatively low atomic percentage is close to that of the detection limit by XPS and thus not significant. There appears to be a small amount of zinc in the Micron CeO_2 sample, the implications and possible causes for this are explored in Appendix 2.

Pour density

In this study, two measurements are taken for each material. The first is the pour or bulk density, which is simply when a known weight of powder is placed in a measuring cylinder and its volume measured. The cylinder is then raised, dropped at a set distance and this process repeated until there is no more reduction in the volume. The volume is re-measured to subsequently estimate the tapped density.

Table 8 shows the results of the pour and the tapped density. The Carr index can thus be calculated from the corresponding bulk and tapped density values using Equation 1:

$$CarrIndex = \frac{TappedDensity - BulkDensity}{TappedDensity} \times 100 \quad (1)$$

The Carr index gives an indication of the powder's flow properties. The smaller the Carr index the better the flow properties (2); Carr index 5-15 indicates excellent flow, 12-16 good, 18-21 fair and 23-28 poor flow.

Table 8. Pour density and tapped density measurement results (and the calculated Carr index); this work was outsourced to Escubed Leeds.

Sample Name	Batch number	Pour (bulk) Density (g/cm^3)	Tapped Density (g/cm^3)	Carr Index	Flow properties as indicated by the Carr index
A. Nanograin CeO_2	CBa250#15	1.121	1.404	20	Fair flow
B. Nanosun ZnO	ZA250#30	1.304	1.523	14	Good-excellent flow
C. Z-COTE HP 1 ZnO	ZB250#64	0.507	0.630	20	Fair flow
D. Micron ZnO	ZrA250#33	0.646	0.714	9	Excellent flow
E. Z-COTE ZnO	ZC250#78	0.415	0.519	20	Fair flow
F. Micron CeO_2	CrA250#40	0.293	0.346	15	Good-excellent flow
G. Ceria dry CeO_2	CA340#13	0.693	0.832	17	Good-fair flow

Comparing the results of pour and tapped densities shows there is a positive correlation between the two, the greater the pour density of the material, the greater its tapped density. The tapped density of a material is always larger than its pour density which is expected as the process of mechanically tapping the sample will result in powder compacting (2).

Dustiness

Dustiness index is a means of quantifying the released dust from the nanomaterial. Table 9 below shows the results for the dustiness of the PROSPEcT sample powders.

Table 9. Mean and SD of the dustiness results (in terms of the inhalable, thoracic and respirable fractions* of dust dispersed) and moisture content of the PROSPEcT sample powders, by the rotating drum method, (outsourced to HSL (Health and Safety Laboratory), Buxton).

Sample Name	Batch number	Inhalable fraction (mg kg^{-1})		Thoracic fraction (mg kg^{-1})		Respirable fraction (mg kg^{-1})		Moisture content (%)	
		Mean	SD	Mean	SD	Mean	SD	Mean	SD
A. Nanograin CeO_2	CBa250#15	2845	244	668	59	66	26	0.4	0.10
B. Nanosun ZnO	ZA250#30	1095	222	317	37	42	8	1.2	0.20
C. Z-COTE HP 1 ZnO	ZB250#64	5880	610	1340	241	138	105	0.3	0.00
D. Micron ZnO	ZrA250#33	166	26	34	10	10	2	0.4	0.10
E. Z-COTE ZnO	ZC250#78	2905	371	599	239	27	3	0.5	0.10
F. Micron CeO_2	CrA250#40	278	9	80	9	22	10	0.2	0.05
G. Ceria dry CeO_2	CA340#13	2222	202	800	11	86	15	1.1	0.10

The powders were also allocated levels of dustiness as defined by the European standard of the dustiness of bulk samples (EN15051) and the corresponding data shown on Table 10.

Table 10. The dustiness classifications of the sample powders, ranging from Very Low to High.

Sample	Dustiness Classification		
	Inhalable	Thoracic	Respirable
A. Nanograin CeO_2	Moderate	Moderate	Moderate
B. Nanosun ZnO	Moderate	Moderate	Low
C. Z-COTE HP1 ZnO	High	High	Moderate
D. Micron ZnO	Very Low	Very Low	Low
E. Z-COTE ZnO	Moderate	Moderate	Low
F. Micron CeO_2	Low	Low	Low
G. Ceria dry CeO_2	Moderate	Moderate	Moderate

2.2.2 Characterisation of nanomaterial in aqueous suspension.

General notes on the results displayed in this section:

a) The four types of liquid media chosen were decided by the University of Exeter within the PROSPEcT consortium. One pre-requisite specified was that no other additives were to be used for the dispersion of the particles. The consensus being that if additives (chemical e.g. detergents, or otherwise) were present in the toxicity testing, then this will influence the results. It is for this reason that NPL did not attempt to disperse the Z-COTE HP1 sample from BASF in aqueous media, due to the hydrophobic silane coating.
b) The results displayed in this section all have the same batch number, as detailed below in Table 11. We will thus use the sample name/supplier information only to refer to the results in this subsection.
c) Unless otherwise specified, all concentrations were made to 50mg/L.

Table 11. Sample information of the PROSPEcT powders used in the characterisation of nanomaterial dispersions in aqueous solution. Sample C, Z-COTE ZnO HP1 is not included in this list.

Sample Name	**Batch number**
A. Nanograin CeO_2	CB250#41#ICP
B. Nanosun ZnO	ZA250#30#ICP
D. Micron ZnO	ZrA250#33#ICP
E. Z-COTE ZnO	ZC250#37#ICP
F. Micron CeO_2	CrA250#40#ICP
G. Ceria dry CeO_2	CA340#13#ICP

Differential centrifugal sedimentation (DCS)

DCS works by measuring the time it takes for injected particles to move from the centre of a spinning disc to the edge where they are detected using a turbidity detector; the larger the particle (for a given density) will mean the shorter the time to reach the edge. One limitation of this technique is that it requires the density of the particle to be accurately known, including any coatings or adsorbed analytes on the surface. Table 12 shows the results of the DCS disc centrifugal sedimentation; D_{10}, D_{50}, D_{90} values (oversize percentiles) are often used to describe the particle size distribution of the sample. If D_{10} = 1225 nm, then this means that that 10 mass % of the particles will have particle diameter of 1225 nm or larger.

Table 12. Disc centrifugal sedimentation results. (a) the measured equivalent spherical particle diameter, the mean and ± SD of 3 replicates are shown. (b) the corresponding D10, D50, D90 values from the averaged DCS measurements.

a)

Sample Name	**DI water (nm)**	**Fish medium (nm)**	**Seawater (nm)**	**Daphnia medium (nm)**
A. Nanograin CeO_2 (Umicore Belgium)	135±4	164±8	187.6±1.7	146±5
B, Nanosun ZnO (Micronisers, Australia)	277±7	390±70	510±40	500±200
D. Micron ZnO (Sigma Aldrich, UK)	590±30	620±20	660±20	631±5
E. Z-COTE ZnO (BASF, Germany)	193±3	290±20	309±10	296±16
F. Micron CeO_2 (Sigma Aldrich, UK)	570±80	530±30	650±80	630±40
G. Ceria dry CeO_2 (Antaria, Australia)	340±50	380±50	520±90	400±30

b)

Sample Name	**DI water (nm)**	**Fish medium (nm)**	**Seawater (nm)**	**Daphnia medium (nm)**
A. Nanograin CeO_2 (Umicore Belgium)	D_{10} 185±2 D_{50} 109±3 D_{90} 73±3	D_{10} 226±9 D_{50} 134±6 D_{90} 89±5	D_{10} 521±3 D_{50} 149.8±0.7 D_{90} 98.3±1.5	D_{10} 200±5 D_{50} 90±60 D_{90} 81±2
B. Nanosun ZnO (Micronisers, Australia)	D_{10} 720±30 D_{50} 40.1±0.7 D_{90} 64.6±0.6	D_{10} 1000±200 D_{50} 190±17 D_{90} 93 ±4	D_{10} 1180±20 D_{50} 330±70 D_{90} 130±50	D_{10} 100±200 D_{50} 400±200 D_{90} 100±50
D. Micron ZnO (Sigma Aldrich, UK)	D_{10} 870±60 D_{50} 572±19 D_{90} 306±7	D_{10} 890±40 D_{50} 606±12 D_{90} 336±8	D_{10} 930±50 D_{50} 639±15 D_{90} 399±14	D_{10} 930±20 D_{50} 612±3 D_{90} 332±6
E. Z-COTE ZnO (BASF, Germany)	D_{10} 286±2 D_{50} 82.8±1.9 D_{90} 107.3±1.7	D_{10} 400±30 D_{50} 270±20 D_{90} 130±30	D_{10} 417±12 D_{50} 301±8 D_{90} 193±7	D_{10} 410±20 D_{50} 285±16 D_{90} 140±30
F. Micron CeO_2 (Sigma Aldrich, UK)	D_{10} 1110 ±150 D_{50} 510±90 D_{90} 158±12	D_{10} 1060±60 D_{50} 470±40 D_{90} 138±6	D_{10} 1160±120 D_{50} 590±70 D_{90} 210±20	D_{10} 1210±60 D_{50} 570±40 D_{90} 163±13
G. Ceria dry CeO_2 (Antaria, Australia)	D_{10} 810±160 D_{50} 202±17 D_{90} 130±60	D_{10} 900±200 D_{50} 231±17 D_{90} 113±4	D_{10} 900±500 D_{50} 400±110 D_{90} 163±14	D_{10} 980±80 D_{50} 230±20 D_{90} 108±3

Results in Table 12 show that the largest mean particle size exists when the nanomaterial is dispersed in seawater; this is reflected in the particle mean size as well as the corresponding D_{90} values. Results also show that the smallest particle size exists when the nanomaterials are dispersed in DI water. Lastly, all of the values recorded are significantly larger than the primary particle size as measured by electron microscopy. This can only be accounted by the fact that particles dispersed in the liquid media do not exists as individual primary particles but in the agglomerated/aggregated form. This is not unexpected as the "as received powders" are already in highly aggregated/agglomerated state (as evident from the electron micrographs). No correlation should thus be made between the primary particle size as measured by the electron microscopy and the particle size measured by DCS as they are measuring two different aspect of particle size information.

Half-Life Measurements

The concept of "half-life" has been put forward in the OECD guidelines as an indication of dispersion stability. Here, half-life is measured from turbidity type measurements and is a function of sedimentation rate. However, half-life measurements here will not only be governed by the surface charge property but also other contributory factor that can result in faster sedimentation e.g. particle size and density of a particular particle type. Thus, turbidity measurements to estimate half-life values are particularly useful when comparing the effects of various media on dispersion stability on a particular particle type. The effect of different media on the sedimentation rate of nanomaterials is summarised on Table 13.

Table 13. Dispersion stability of PROSPEcT powders as measured by their "half-lives".

Sample Name	DI water (min)	Fish medium (min)	Seawater (min)	Daphnia medium (min)
A. Nanograin CeO_2	2676	282	288	252
B. Nanosun ZnO	2526	498	402	444
D. Micron ZnO	966	216	228	324
E. Z-COTE ZnO	4038	816	738	768
F. Micron CeO_2	432	348	294	294
G. Ceria dry CeO_2	780	438	534	600

Generally, results show that nanomaterials are most stable when dispersed in DI water and least stable when in an ecotox medium. The results for the larger *Micron* size particle (i.e. Micron ZnO and Micron CeO2), show that these particles sediment out fastest as reflected by their small half-life values.

Zeta Potential

Another method of determining dispersion stability is through the estimation of zeta-potential values. Zeta-potential gives an indication of the electrostatic repulsion forces between particles, in which a high plus or minus zeta potential will mean an increase in this repulsion, to render a more stable dispersion as the particles are less inclined to agglomerate/aggregate. Zeta-potential measurements will solely be governed by the electric properties of solid surface in contact with liquid. The measured zeta-potential values for the PROSPEcT nanomaterials are summarised in Table 14.

Table 14. The mean values of zeta-potential (of six replicates) for different PROSPEcT nanomaterials dispersed in various media at a concentration of 50 mg/L.
*** DI water + 5 mM NaCl - this medium was employed to compare with the DI results when in the presence of inert background electrolyte. Values are the mean and +/- 1 SD of six replicates. Refer to Table 12 for batch number assignment.**

Sample Name	DI water (mV)	DI water + 5mM NaCl* (mV)	Fish medium (mV)	Seawater (mV)	Daphnia medium (mV)
A. Nanograin CeO_2 (Umicore Belgium)	33±2	33.9±1.7	-11.1± 1.0	N/A	1.2± 0.2
B. Nanosun ZnO (Micronisers, Australia)	24.6 ±0.4	25.2±0.6	12.4±0.3	N/A	4.9± 0.2
D. Micron ZnO (Sigma Aldrich, UK)	20.2±0.4	13.9±0.6	4.4±0.4	N/A	-4.6± 0.4
E. Z-COTE ZnO (BASF, Germany)	24.3±0.4	20.8±0.8	10.8±0.1	N/A	1.3± 0.2
F. Micron CeO_2 (Sigma Aldrich, UK)	-7±6	-2±2	-22.3±0.5	N/A	-15.0± 0.3
G. Ceria dry CeO_2 (Antaria, Australia)	28±2	23.0±1.3	-15.3±0.6	N/A	-17.4 ± 0.3

The zeta-potential values of nanomaterials when dispersed in seawater cannot be successfully measured (due to high conductivity) and thus displayed as N/A in the table. In general, results indicate high zeta-potential values for nanomaterials that are dispersed either in DI water (or more reliably DI water + 5 mM NaCl) than in corresponding ecotox media; the use of NaCl in the dispersing media confers the stability measurement in DI water. This is true apart from Micron CeO_2 where dispersion in DI resulted in the least stable dispersion.

Inductively-coupled Plasma Mass Spectrometry (ICP-MS)

ICP-MS is an analytical technique used for elemental detection with limits in the ng/g range. Table 15 shows the ICP-MS results for the measurement of dissolution of CeO_2 PROSPEcT nanomaterials dispersed in the four different liquid media. Table 16 shows the corresponding ZnO results. In both cases, the nanomaterial dispersions were stored in the fridge after day 2 in order to prevent degradation of the sample. Prior to the extraction of the supernatant, each of the 1-L bottles were shaken gently to ensure that the aliquoted sample was representative. The dissolution study was conducted over a period of 21 days. The concentration of zinc and cerium in the corresponding blank media (i.e. with no nanomaterials) is tabulated in Table 17.

Table 15. The dissolution results of the CeO_2 PROSPEcT powders (in four different media) using ICP-MS (of the extracted supernatant solutions) over time.

Type of media	Day	Cerium concentration of the supernatant extracted (ng g^{-1})		
		Nanograin Ceria (Umicore, Belgium)	Micron CeO_2 (Sigma Aldrich, UK)	Ceria dry CeO_2 (Antaria, Australia)
DI water	2	2.49	sample missing	1.67
	6	2.9	1.88	1.83
	9	1.94	1.05	2.06
	14	5.08	1.79	1.87
	21	1.59	1.33	2.7
Fish	2	1.09	1.55	1
	6	1.72	2.61	1.75
	9	2.22	3.96	2.37
	14	1.57	1.42	1.9
	21	1.58	1.35	3.1
Daphnia	2	1.91	1.78	sample missing
	6	2.02	1.93	1.68
	9	1.7	1.43	sample missing
	14	1.68	1.92	1.62
	21	1.64	3.45	22.4
Seawater	2	1.92	2.01	1.22
	6	3.95	5.76	4.83
	9	1.88	3.17	4.76
	14	1.97	6.09	5.92
	21	2.19	2.52	9.23

Table 16. The dissolution results of the ZnO PROSPEcT powders (in four different media) using ICP-MS (of the extracted supernatant solutions) over time.

Type of media	Day	Zinc concentration of the supernatant extracted (ng g^{-1})		
		Nanosun ZnO (Micronisers, Australia)	Micron ZnO (Sigma Aldrich, UK)	Z-COTE ZnO (BASF, Germany)
DI water	2	764	1864	2536
	6	1741	3436	3360
	9	1490	2813	3130
	14	1808	3005	3772
	22	1607	6007	5030
Fish	2	1198	1780	2216
	6	1632	2442	2192
	9	1744	2420	3028
	14	1676	2961	2697
	22	1954	3239	3036
Daphnia	2	1158	1465	1454
	6	1458	1644	sample missing
	9	1731	1515	1014
	14	1052	2193	1588
	22	1402	2611	2037
Seawater	2	241	531	681
	6	371	466	736
	9	439	605	773
	14	420	1089	972
	22	359	1051	1155

Table 17. ICP-MS data for the concentration of zinc and cerium in the four different media.

Media blanks	Zn concentration (ng g^{-1})	Cerium concentration (ng g^{-1})
DI water	11.9	1.38
Fish medium	22.9	1.5
Seawater medium	59.6	1.57
Daphnia medium	23.3	1.43

Results show that CeO_2 dissolution (Table 15) is not apparent, in that the levels of cerium is estimated to be below ~ 20 ng/g in all media over a 21 day period and no more than in the seen corresponding control samples. Zinc oxide dissolution (Table 16) is much higher throughout, with an apparent increase in the amount of dissolved zinc through time with DI water; this is not surprising, as the dissolution behavior of ZnO nanomaterial is well known in the nano(eco)tox community. Overall, in the case of ZnO, the rate of dissolution is slowest in seawater; this observation was consistent with the colorimetry test results documented in the previous NPL Interim Report. It is thought that the much larger ionic concentration found in seawater can inversely affect dissolution rate, possibly through the ability to influence *inner–sphere adsorption*, which have been known to be important in mineral dissolution (3).

Photocatalytic properties

This study was conducted to determine the ability of the nanomaterials to generate reactive oxygen species (ROS), including radicals, under photocatalytic conditions. When metal oxide nanoparticles are irradiated with electromagnetic radiation with photon energy is greater than the band gap, electron-hole pairs are generated. TiO_2, ZnO and CeO_2 have band-gaps between 3.1 eV and 3.3 eV, which means electron-hole pairs can be generated by irradiation with UV light from the sun. The electrons and holes that diffuse to the nanoparticle surface have the ability to respectively reduce and oxidize molecules adsorbed onto this surface. In particular, the reduction of oxygen molecules leads to the production of $\cdot O_2^-$, whose further reduction generates other ROS such as H_2O_2. The holes have the ability to directly oxidize molecules in the surroundings, including hydroxide ions generating ·OH radicals. Figure 3 summarises the indirect measurement of ROS formation under photocatalytic conditions, using a potassium iodide probe. When iodide anions are oxidized, tri-iodide anions form, which exhibit a typical yellow colour and an optical absorption peak at 352 nm. Anatase TiO_2 dispersed in the four different media was used as positive control; media with no nanomaterials were used as a negative control. The values are normalized to the absorption measured for the negative control in DI water.

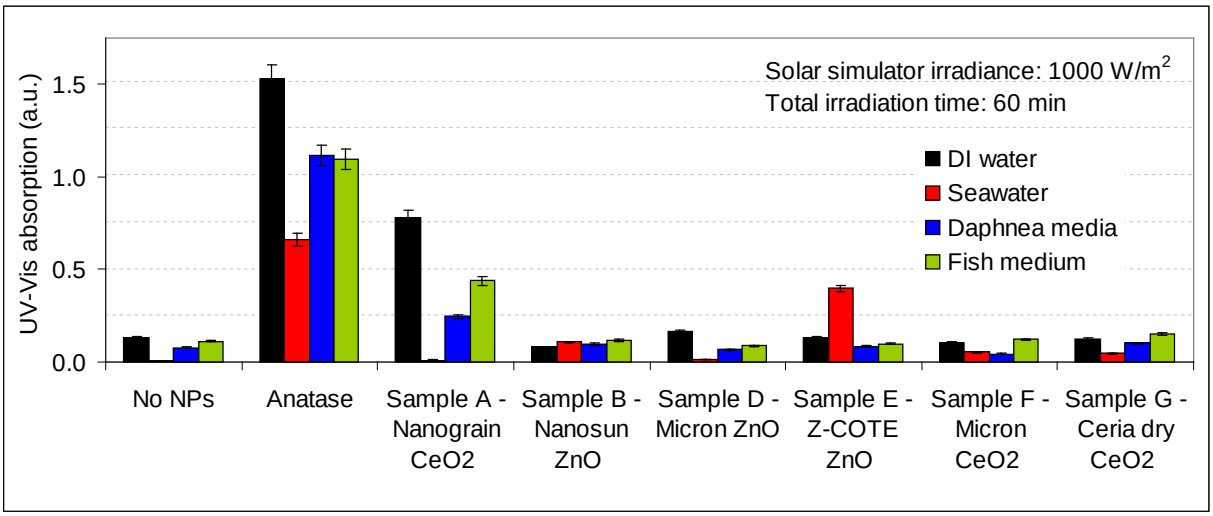

Figure 3. Absorbance readings, at 352 nm, of PROSPEcT nanomaterials in different media (DI water, seawater, daphnia and fish) after being irradiated with solar simulator at 1000 W/m^2 for 60 minutes, as compared with Anatase TiO_2 nanomaterial (supplied by Sigma Aldrich, UK). Refer to Table 12 for batch number assignment.

Results show that there was a small amount of tri-iodide (I_3^-) measured in the irradiated samples containing media only. Interestingly, tri-iodide was suppressed in seawater. Results for Anatase (TiO_2), being the most active photocatalytic material, show a much higher rate of tri-iodide formation than the PROSPEcT nanomaterials. The absorbance signal was highest in DI water, the medium with the least concentration of ionic species. When in seawater, the absorbance signal was reduced (as in the corresponding control i.e. seawater with no Anatase). Several possible reasons can be attributed to what is being observed when in seawater: a) presence of scavengers b) enhanced aggregation/sedimentation of the nanomaterials. Out of all the PROSPEcT nanomaterials, Nanograin CeO_2 displays the closest behaviour to Anatase, in having the largest absorbance signal in DI water and the smallest when in seawater. Among the PROSPEcT nanomaterials which have the smallest primary particle size, Nanograin CeO_2 exhibits the highest photocatalytic ability (see Tables 1, 2 and 13) suggesting that the photocatalytic ability increases with decreasing size. Z-COTE ZnO is interesting, in that it does not follow a similar pattern observed with Anatase and Nanograin CeO_2. With Z-COTE ZnO, the absorbance signal is much higher in seawater than when dispersed in the other three media and at present no explanation for this can be provided. With the other PROSPEcT nanomaterials, the

absorbance signals were within a similar range to that of the corresponding irradiated negative control. Samples that were kept in the dark exhibited no absorption peak at 352 nm. Lastly, a UV-visible plate reader was used to follow the cumulative production of I_3^- with varying irradiation time, as quantified by measuring absorption at 352 nm. In summary, results (not shown here) show that absorbance signal generally increases with irradiation time and this can be attributed to the increase in the amount of ROS being generated. Again, our findings are consistent with previous observations, in that:

a) Anatase gave the highest absorbance reading.
b) Nanograin CeO_2 gave a similar trend to Anatase i.e. largest absorbance reading in DI water and lowest when in seawater. This is also the materials smaller in size.
c) Z-COTE ZnO gave a higher absorbance reading in seawater than when in other media.

The photocatalytic behaviour of the PROSPEcT powders was further studied by measuring the production of specific ROS (results not shown here). By using molecular probes with tailored optical properties, we assessed the photo-production of superoxide radicals, hydrogen peroxide and hydroxyl radicals. Controlled experiments confirmed that the particles catalyzed photo-oxidation and photo-production of ROS, while no ROS generation was observed when the ionic form of the materials was used in place of the particles. While affecting their aggregation and sedimentation, the type of media was not found to strongly influence the photo-catalytic behaviour of the particles. Within the size range that was investigated, ZnO particles resulted in the highest production of specific ROS.

Redox Potential

As indicated in the OECD guidelines, redox potential (ORP) measures the potential difference across two electrodes: a Pt electrode against a double junction Ag/AgCl reference electrode, when immersed in the nanomaterial dispersion. Table 18 shows the redox potential results associated with dispersions of the PROSPEcT nanomaterials in four different media; the table also contains the redox potential value of the corresponding blank media - liquid media with no nanomaterial. Figure 4 shows the corresponding bar chart of these results.

Table 18. Redox potential of nanomaterial dispersion in various liquid media. The value quoted (in mV) is relative to the standard hydrogen reference electrode. Refer to Table 12 for batch number assignment.

Sample Name	Redox potential (mV) of nanomaterial dispersions			
	DI water	Fish medium	Seawater	Daphnia medium
Liquid media with no nanomaterials	405	418	384	425
A. Nanograin CeO_2 (Umicore Belgium)	416	439	384	415
B. Nanosun ZnO (Micronisers, Australia)	398	424	380	415
D. Micron ZnO (Sigma Aldrich, UK)	398	430	374	415
E. Z-COTE ZnO (BASF, Germany)	396	427	379	422
F. Micron CeO_2 (Sigma Aldrich, UK)	422	430	382	429
G. Ceria dry CeO_2 (Antaria, Australia)	414	436	387	426

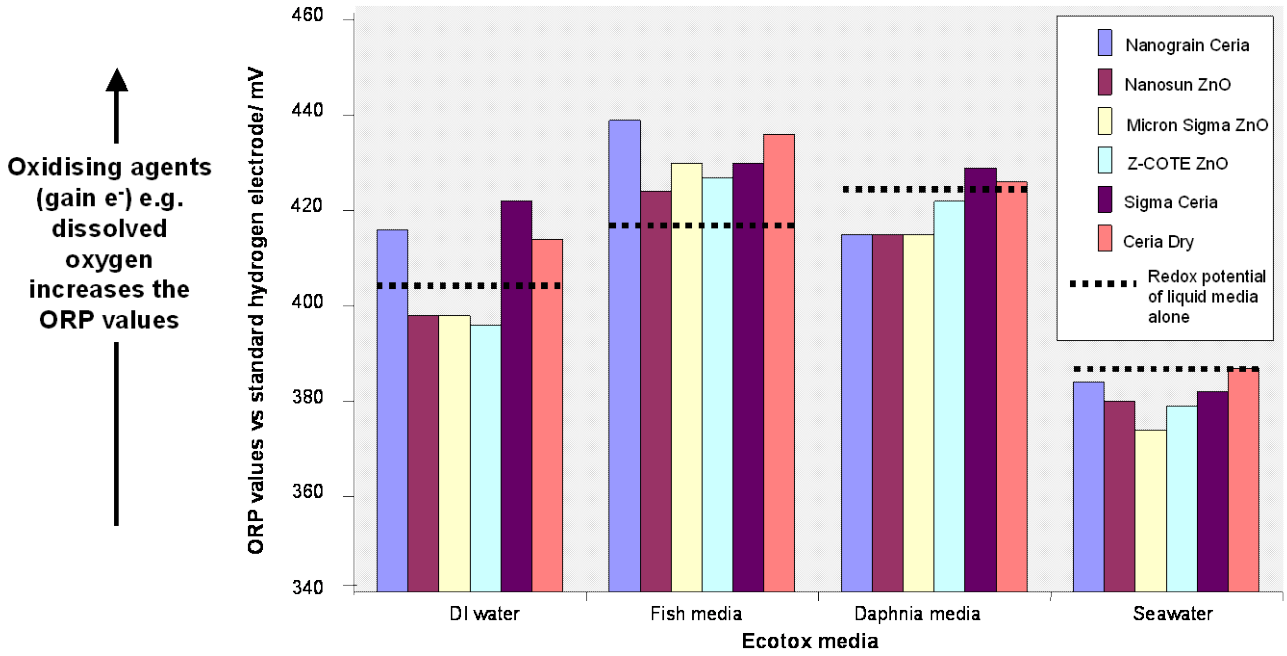

Figure 4. Graphs of redox potential results summarized in Table 19. Refer to Table 12 for batch number assignment.

Results show that ORP values are dominated by the type of liquid media used for dispersions, with seawater resulting in smallest values compared to other media. The ORP values reported here are not specific to a single chemical species and thus represent an aggregate oxidization-reduction of all species that can interact at the platinum working electrode. The fact that the type of liquid media itself seems to have some contribution to the final ORP values is not surprising, as dissolved redox species in the liquid can easily interact with the Pt electrode of the ORP probe. In fact, such ORP measurements are often employed as an accurate gauge of water quality and the monitoring of dissolved species in the water. Seawater in particular is shown to be more reducing in nature if compared to the other liquid media; this is mainly due to the higher concentration of reducing agents (such as NO_2^-) in seawater. The presence of such reducing agents has the effect of lowering the ORP value. Furthermore, we expect a much reduced level of oxidising agent such as dissolved oxygen in such a high saline solution i.e. the higher the salinity, the less oxygen the water can hold. If there is a reduction in oxidising agents then this also has an effect to lowering the ORP value. It must be stressed however that although the redox potential values acquired from the ORP electrode may be indicative of the redox state of the system as a whole i.e. measuring the ability of oxidisers or reducers (in solution) in a given system, it is difficult to know the redox potential contribution (or lack of) from the particles themselves, which could render the technique as being unsuitable.

2.2.3 Characterisation of aerosolised nanomaterial powders

Table 19 shows the Geometric Mean particle sizes and the Geometric Standard Deviation of the different aerosolised PROSPEcT powders as measured by the scanning mobility particle sizer (SMPS). Aerosolisation was performed on the *as received* powders. Size distribution plots for all the samples have been uploaded to the NAPIRA database; the data has been corrected for any source drift using the particle number concentration data from a standalone condensation particle counter (CPC). A log-normal curve was fitted to the size distribution data plots to calculate the geometric mean and standard deviation. Each plot represents the mean values of at least 6 SMPS scans of 200 seconds each. The mean particle diameter results range from 225 nm – 400 nm.

Table 19. Geometric Mean particle sizes and Geometric Standard Deviation values of the different aerosolised PROSPEcT powders, as measured by SMPS.

Sample Name	Supplier	Batch Numbers	Geometric Mean Particle Size	Geometric Standard Deviation of log-normal
A. Nanograin CeO_2	Umicore Belgium	NM-212 06035, 06037, 06038	359nm	1.66
B. Nanosun ZnO	Micronisers, Australia	NM-112 06022, 06023, 06024	269nm	1.80
C. Z-COTE HP1 ZnO	BASF, Germany	NM-111 06298	400nm	1.57
D. Micron ZnO	Sigma Aldrich, UK	NM-113 06032, 06033, 06034	300nm	1.63
E. Z-COTE ZnO	BASF, Germany	NM-110 06309	289nm	1.68
F. Micron CeO_2	Sigma Aldrich, UK	NM-213 06043, 06045, 06046	233nm	1.63
G. Ceria dry CeO_2	Antaria, Australia	NM-211 06031, 06032, 06033	225nm	1.77

If these values are compared to the equivalent DCS particle size (when the powders were dispersed in solution) and electron microscopy particle size (performed on powder samples), then it is apparent that there is no relationship between them. The lack of relationship of particle size information as analysed by various techniques is not surprising, as the following factors will contribute to the discrepancies:

a) The different methods of handling/dispersing the particles and how the particle size information was acquired by the instrument
b) Different inter-particle interaction forces; in a liquid dispersion, the colloidal suspension may confer stability via electrostatic interactions, which will not be present in an atmospheric aerosol sample.

CHAPTER 3. SUMMARY AND FUTURE WORK

This report describes the output of the physico-chemical characterisation studies under the PROSPEcT project. The main outputs are the:

a) Test results from the ZnO and CeO_2 nanomaterials
b) Research findings surrounding measurement issues and the developing new measurement platforms/ tools for nanomaterial characterisation.

Core Activities

It has been demonstrated that as with most powders, particle size information has a direct influence on other parameters such as surface area, dispersion stability and dissolution kinetics, indicating the need to accurately measure this parameter. The importance of particle size as a parameter also coincides with the general consensus amongst the nano(eco)tox community in that size is a key factor in determining the toxicity of a particle i.e. the smaller the particle the more toxic it becomes. This is due to properties such as the ease of penetration through the cell membrane and high surface area. Having said this, it may be argued that size is not the only factor influencing nanotoxicity and it will be important to measure other parameters as identified by this OECD initiative; the disadvantage here is that an exhaustive list of parameters will mean the inability to conduct economically viable tests. In order to reduce the number of parameters required for testing, it is crucial to find relationships and quantify the degree of correlation between the physicochemical parameters and toxicity endpoints. This can only be achieved objectively using data mining methods.

Additional Studies

Our work has included activities in order to tackle measurement issues that exist in nanomaterial research. Our aim here is to:

a) understand where measurement variability could arise (potentially introducing error or bias in the measurement).
b) develop new measurement methods; this work is still on-going and currently funded under different projects.
c) to verify the homogeneity of subsampled samples for potential future use as reference material.

Our findings have shown that variability in the data can arise from protocol variability or the lack of understanding on the limitations of the various tools employed by the operator. The solution here is to have validated methods for the purpose of standardisation.

Future Directions

Over recent years we have learned a great deal about nanomaterial characterisation in a nano(eco)toxicological context, and our biggest challenge is to understand what and how to measure in order to achieve the desired level of accuracy and reproducibility. As schematically shown in the figure below (Figure 5), major roadblocks exists and are due to: the lack of suitable reference materials and making reliable/accurate measurements under challenging conditions. Research associated with development of better tools is currently lagging behind and the community is awaiting the emergence of new technologies. For example, the majority of techniques used assume that particles are spherical and often this is not the case. This difficulty is compounded by the fact that the nanomaterial, when dispersed in a nano(eco)tox media will often result in an unstable dispersion. Furthermore, as schematically shown in Figure 6, the fate of the nanomaterial in the dispersion can take different (multiple) pathways to include: aggregation, deposition, sorption/desorption, etc. It is the dynamic nature of how particles and their interaction with the liquid environment that is often so difficult to capture and measure.

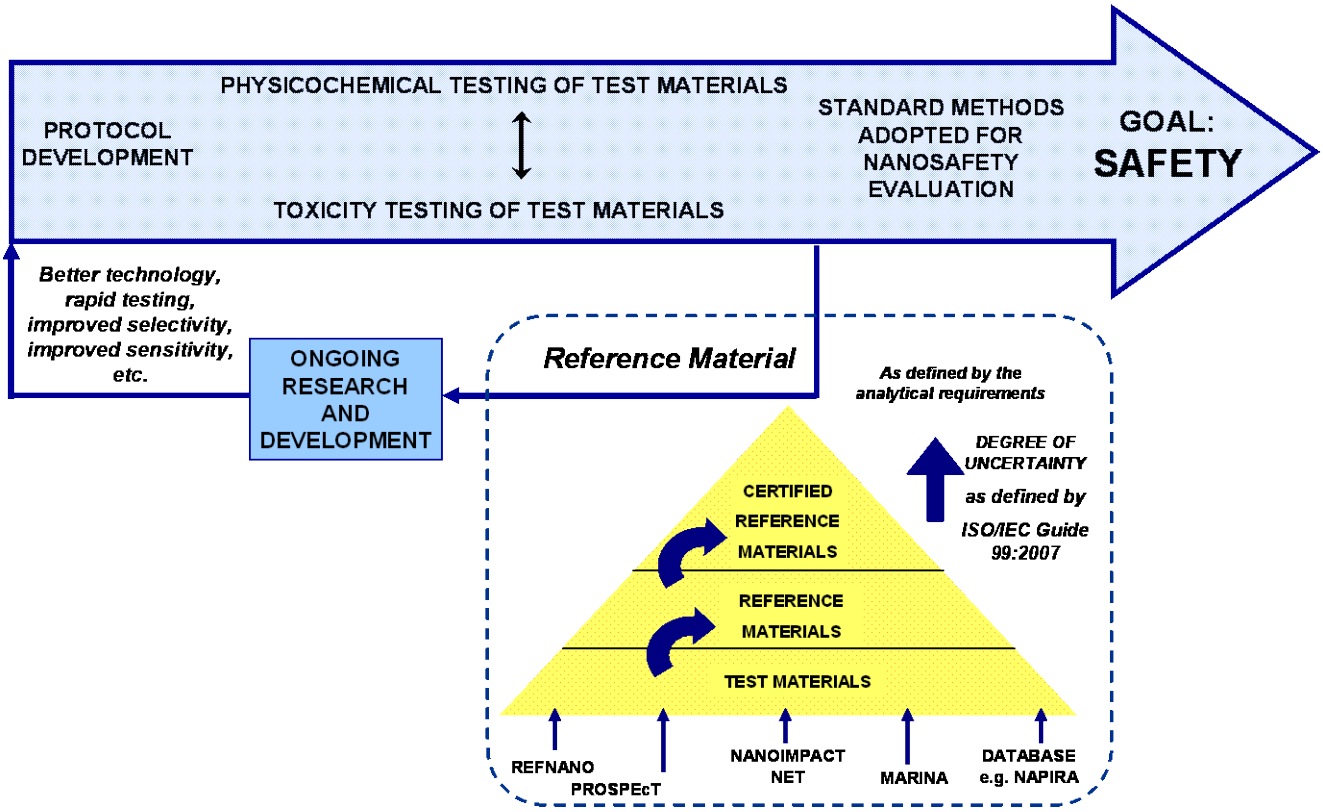

Figure 5. Schematic diagram showing the ever changing landscape of nanomaterial research in nano(eco)toxicity, a roadblock in standardisation.

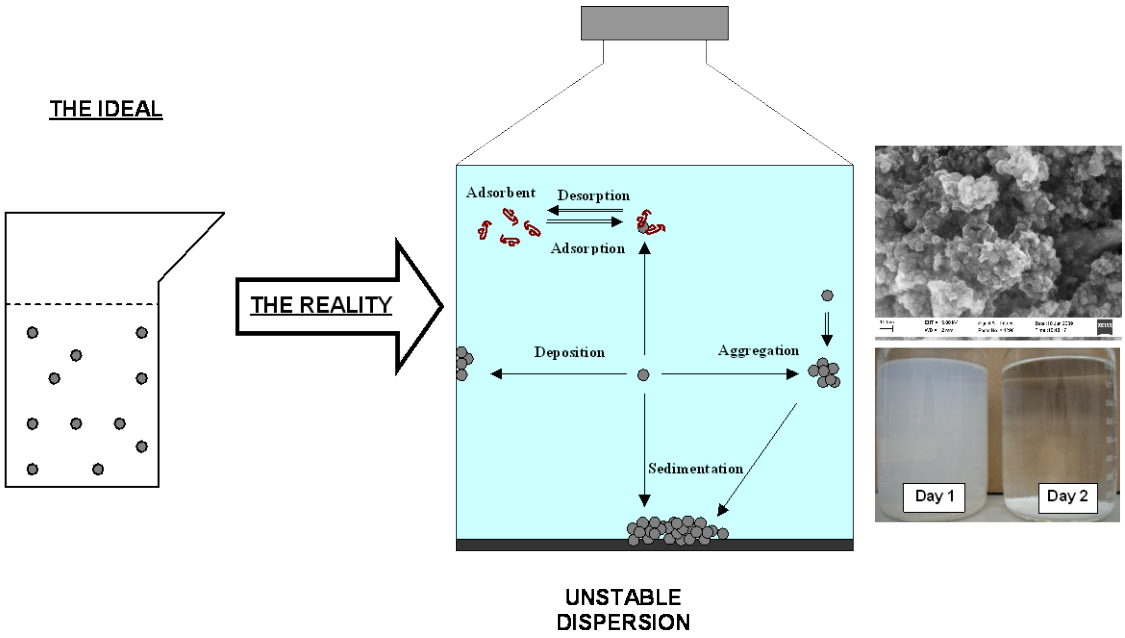

Figure 6. Characterisation of the non-ideal sample using current tools, to include non-sphericity of the nanomaterial and unstable dispersions.

As the goal of the project is safety, it is logical to ask: *under what conditions do nanomaterials become toxic,* rather than asking: *are nanomaterials toxic?* Only then can we identify the risks posed by the nanomaterial under study. In order to answer the former question, there is a need for high-throughput tools, such that the tests can be performed under various conditions. The power of high-throughput analysis is in its ability to screen how the property of a particular nanomaterial can change under many different conditions. It is envisaged that should a high-throughput tool exist, then the information gained from such a platform would feed in to help design better nano(eco)tox type tests.

ACKNOWLEDGEMENTS

We acknowledge expert advice received from: Andy Wain, Nick Walker, Richard Shaw, Alex Shard, Neil Harrison, Vince Hackley (NIST), University of Exeter and University of Surrey. This work was conducted as part of PROSPEcT, which is a public-private partnership between DEFRA, EPSRC and TSB and the Nanotechnology Industries Association (NIA Ltd.) and its members, and was administered by the DEFRA LINK Programme.

REFERENCES

1. Protocol for Nanoparticle Dispersion [Internet]. Available from: http://www.nanotechia-prospect.org/managed_assets/files/prospect_dispersion_protocol.pdf

2. Particle & Powder Density, Hausner Index and Carr Ratio [Internet]. Available from: http://www.escubed.co.uk/sites/default/files/density_measurement_(006)_carrs_index_and_hausner_ratio.pdf

3. Johnson SB, Yoon TH, Kocar BD, Brown GE. Adsorption of Organic Matter at Mineral/Water Interfaces. 2. Outer-Sphere Adsorption of Maleate and Implications for Dissolution Processes. Langmuir. 2004;20(12):4996–5006.

4. Tantra R, Jing S, Gohil D. Technical issues surrounding the preparation, characterisation and testing of nanoparticles for ecotoxicological studies [Internet]. 2010 [cited 2012 Feb 6]. p. 165–76.Available from: http://library.witpress.com/viewpaper.asp?pcode=ETOX10-016-1

5. Tantra R, Jing S, Pichaimuthu SK, Walker N, Noble J, Hackley VA. Dispersion stability of nanoparticles in ecotoxicological investigations: the need for adequate measurement tools. Journal of Nanoparticle Research. 2011 Feb 26;13(9):3765–80.

6. Seah MP. Topography effects and monatomic ion sputtering of undulating surfaces, particles and large nanoparticles: Sputtering yields, effective sputter rates and topography evolution. Surface and Interface Analysis. 2012 Feb;44(2):208–18.

APPENDIX 1: DISSEMINATION ACTIVITIES

It is outside the scope of this report to describe in detail all of the accomplishments that we have achieved under the PROSPEcT project and the success of this project hinges on our extensive dissemination activities. Where possible the work has been disseminated either through formal scientific publications and oral presentations at conferences. A full list of our dissemination activities is shown in Table 20. Activities are subdivided into three activities as published: on the NIA website (http://www.nanotechia-prospect.org/publications/basic), through peer review journals and through attendance of international conferences.

Table 20. A summary of dissemination activities under the PROSPEcT programme: a) through NIA website b) through peer reviewed journal c) through attendance international conferences.

a)

Method/ Format of dissemination	Title	Stage of Completion
Report	Protocol for Nanoparticle Dispersion	Completed
Report	Guidelines and Protocol for Sampling	Completed
Report	Evaluation and Assignment of Nanoparticle Dispersion/ Characterisation Methodologies, to be Developed under PROSPEcT	Completed
Video	Video: Dispersion Protocol	Completed

b)

Journal article details	Stage of Completion
R.Tantra et al. Technical issues surrounding the preparation, characterization and testing of nanoparticles for ecotoxicological studies, Environmental Toxicology 3, WIT Transactions on Ecology and the Environment, 132 (2010) 165-176.	Published
R. Tantra, et al. Nanoparticle characterisation for ecotoxicological studies using Dynamic Light Scattering, Scanning Electron Microscopy and Nanoparticle Tracking Analysis Techniques. The International Journal of Sustainable Development and Planning, 6, (2011) 212–225	Invited, Published
R. Tantra, et al. Dispersion Stability of Nanoparticles in Ecotoxicological Investigations: the Need for Adequate Measurement Tools, Journal of Nanoparticle Research. 13, (2011) , 3765-3780.	Published
M.P Seah Topography Effects and Monatomic Ion Sputtering of Undulating Surfaces, Particles and Large Nanoparticles: Sputtering Yields, Effective Sputter Rates and Topography Evolution, Surface and Interface Analysis, *in press* 2011	Available on-line
R.Tantra, et al. Measurement of Redox Potential in Nanoectoxicological Investigations, Journal of Toxicology, 2011 available on-line	Available on-line
C. Minelli, et al. Metal oxide particles catalyze photo-oxidation and production of reactive oxygen species in environmental media, submitted.	Submitted

c)

Activity type	Details	Stage of Completion
Oral presentation, invited	R. Tantra Institute of Physics, London 28 June 2009, Metrology and Characterisation of Nanoparticles, Nanoparticle Research at NPL: Past, Present and Future.	Completed
Oral presentation	R. Tantra Environmental Toxicology 3, Cyprus 4-6the May, 2010 Technical Issues Surrounding the Preparation, Characterisation and Testing of Nanoparticles for Ecotoxicological studies.	Completed
Oral presentation	R. Tantra Pacifichem, Honolulu 15- 20 December 2010, Nanoparticle Characterisation in Ecotoxicological Media: the Role of Reference Material and Document Standards.	Completed
Oral Presentation	J. Lee SIMS Europe, Muenster, Germany, 19-21 September 2010. Also presented at a different meeting: AVS 57 International Symposium, Albuquerque, NM, USA, 17-22 October 2010. Fundamental Sputtering Yields of Nanoparticles Using SIMS.	Completed
Oral Presentation and course	C. Minelli SETAC Europe 21st Annual Meeting, Milan 15 – 19 May, 2011. Characterisation of ZnO and CeO_2 in the Framework of an Ecotoxicological Study. A course on Characterisation of Nanoparticles in the Framework of Ecotoxicology Studies was also delivered at the same conference.	Completed
Oral Presentation, invited	R. Tantra NANO-S&T, Dailin, China, October 23-26, 2011. Physicochemical Characterisation in Nanotoxicological Research: Current Challenges and Future Opportunities	Completed
Oral Presentation	R. Tantra SETAC North America 32nd Annual Meeting, Boston, USA, 13–17th November, 2011, Metrology Tools for Studying the Behaviour and Effects of Nanomaterials in the Environment and Biological Systems	Completed
Poster at conference	J.Lee, et al. 14th International Conference on Applications of Surfaces and Interface Analysis (ECASIA'11) Cardiff, UK, 4-9 September 2011. A fundamental study of sputtering yields of gold nanoparticles	Completed

Poster at conference	C. Minelli 6th International Conference on the Environmental Effects of nanoparticles and nanomaterials, London (UK), 19-21 September 2011 Assessment of production of reactive oxygen species (ROS) photocatalyzed by metal oxide nanoparticles,	Completed

APPENDIX 2: FURTHER STUDIES

1. SOURCES OF VARIABILITY IN MEASUREMENTS

One of the main challenges in nano(eco)toxicological investigations is the selection of suitable measurement methods and protocols for nanomaterial characterisation in order to obtain accurate and reliable data. Thus, the purpose of the study presented in this section is to understand the potential sources of inaccuracy and the factors that may contribute to data variability and measurement error, which may explain any observed differences between different testing laboratories. Some of the factors are highlighted below:

Dispersion of powders into liquid suspension

Although relatively simple to conduct, it is important not to trivialise this initial step, as this has been shown to have an effect on particle size distribution. Figure 7 gives the DLS particle size distribution of Nanograin CeO_2 (50 mg/L) in DI water when different probes were used for dispersing. If an ultrasonic probe is used, the particle distribution ranges from 68 - 615 nm in size. However, the particle size distribution becomes much broader when either an overhead stirrer or homogeniser is employed instead. This behaviour can be attributed to the lower shear energy provided by these latter probes, which are potentially insufficient to cause de-agglomeration/de-aggregation of the primary particles.

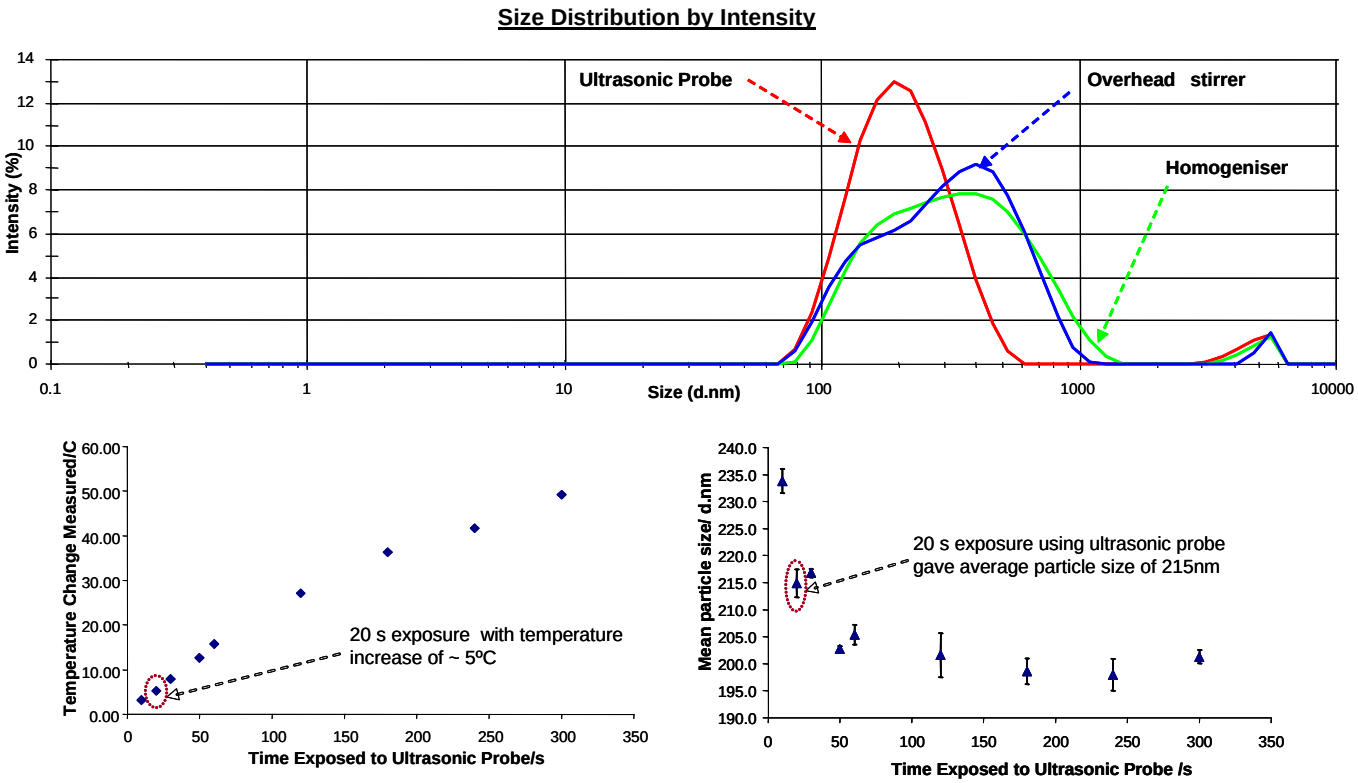

Figure 7. Particle size distribution of CeO_2 in DI water (50 mg/L) and the effects of using different de-agglomeration tools (with "exposure time" of 1 minute). The Figure also shows the effect of varying "exposure time" (using an ultrasonic probe) on the DLS mean particle size of CeO_2 in DI water (50 mg/L) of: corresponding temperature change measured in the dispersion and the corresponding DLS mean particle size.

Figure 7 shows that changing the exposure time will not only have an effect on particle size but also on temperature of the dispersion. Results show that particle size decreases (up to a certain limit) and dispersion temperature increases with an increase in exposure time. The need to have well-controlled protocols on dispersion, which must be agreed by the various stakeholders in the research community, is clear and should an operator decide not to follow a particular protocol step, then this could affect the end result. For further details of this study, please refer to our published paper elsewhere (4).

Unstable dispersions

It is difficult to perform accurate and reliable measurements with current tools if the nanoparticle dispersion under analysis is not stable. Some routine tools, such as DLS, are incredibly sensitive to changes in the dispersions. Figure 8 shows visually a sedimentation experiment, clearly indicating the PROSPEcT nanomaterial dispersion made in an ecotox fish medium is less stable compared to when dispersed in de-ionised water. The stability of these dispersions was monitored for a period of three days using various techniques, including DLS and Micro-Doppler Electrophoresis (for zeta-potential measurements). Data points of the fish media dispersion after day 1 are considered to be unreliable because the low particle concentrations which resulted in a poor signal-to-noise ratio. It is important to establish the limit of quantification for each technique employed for the nanomaterial under analysis, as nano(eco)toxicological investigations often require the need to conduct analysis at extremely low particle concentrations, nanograms per litre (ng/L) or less. We have conducted several experiments to establish the concentration of choice (50 mg/L) used for our nanomaterial characterisation in the PROSPEcT project (5).

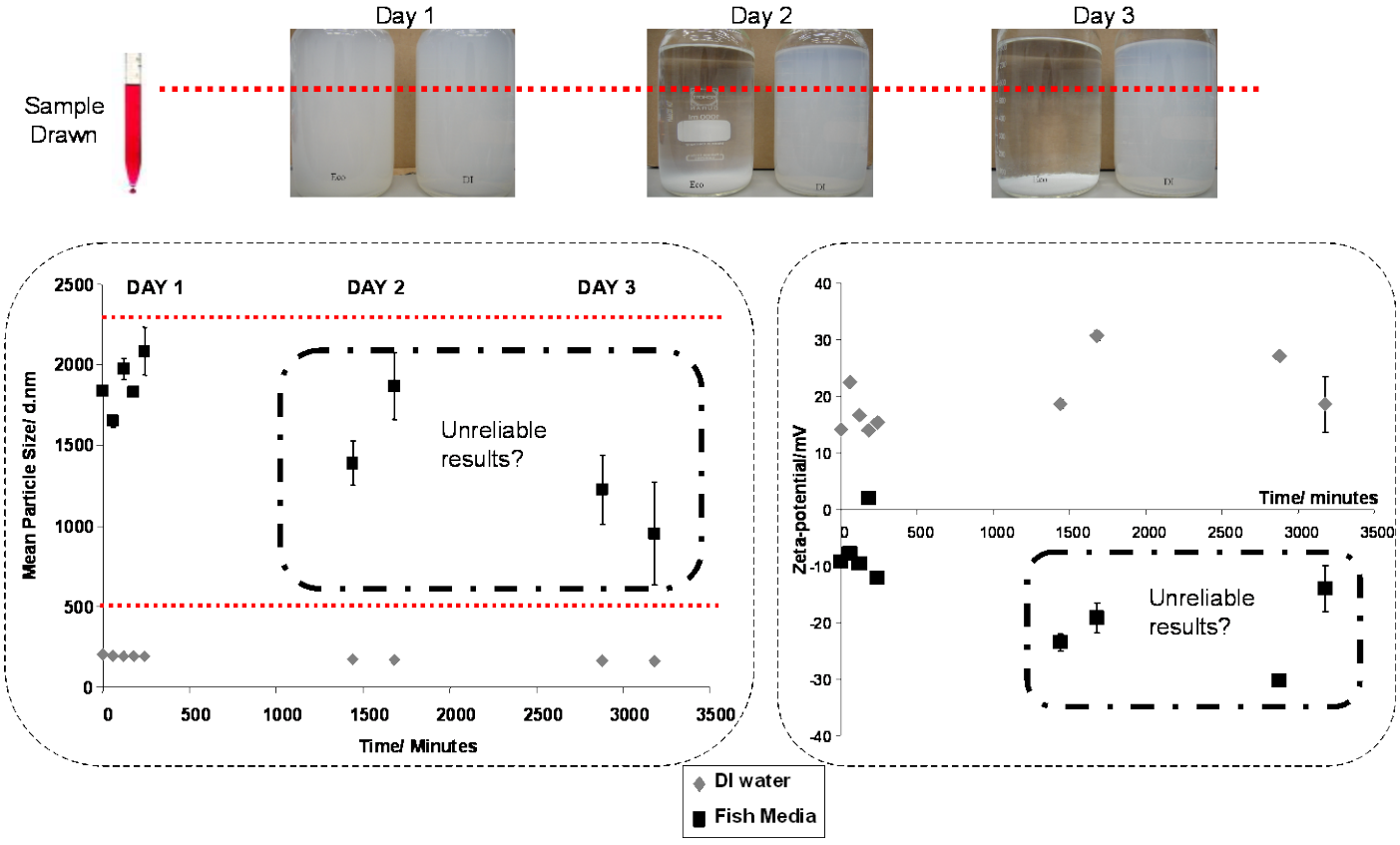

Figure 8. Zeta-potential and DLS mean particle size of CeO_2 (50 mg/L) dispersed in fish media vs. DI water, and sampled at various intervals during a three-day dispersion stability study, with error bars of one standard deviation.

Subsampling issue: To Scoop Sample or Spin-riffled?

The PROSPEcT consortium held discussions concerning the best way on how to subsample the powders, with some partners employing the scoop sampling as opposed to the spin riffling method. Although guidelines on sampling have been published elsewhere (1), these guidelines were based on the sampling of micron sized (and larger) particles, as opposed to nanomaterials. Some members in the consortium felt that powders such as Z-COTE HP1, due their coating of silane, will not be suitable to be spin riffled (as the silane coating prevented the powder to be free-flowing in nature).

Although spin riffling has not been sufficiently validated to show that it is indeed *fit for purpose* for each of the individual powders, it is the only technique that can practically divide large amounts (kgs) worth of nanomaterial powders into smaller (<2g) aliquots. In an attempt to have some estimate on how factors (such as subsampling methods and powder deterioration through time) can have an effect on data quality, we have compared BET data on powders aliquoted from scoop sampling as oppose to the spin riffled method. Table 21 below shows the results of BET measurements of two powders Z-COTE HP1 and Z-COTE; the ZnO powders were supplied by BASF, Germany. Results show the different BET SSA results when the powders were subsampled by the scoop sampling method compared to the spin riffled method. The former results were acquired using the BET instrument at NPL at the beginning of project (this was conducted for the purpose of characterisation of the PROSPEcT powders for WPMN OECD drive) and the latter was acquired using BET equipment at MCA Services towards the end of the project (this was conducted as part of the homogeneity testing study for JRC).

Table 21. Summary of the specific surface area values for PROSPEcT powders, as obtained by the BET gas adsorption technique, comparing results when samples were subsampled using the spin riffled method as oppose to the scoop sampling method.

BASF powder samples – NM111 - Z-COTE HP 1 ZnO, BASF Germany				
Operator/Instrument manufacturer	**Subsampling description/batch number**	**Relative time of analysis**	**SubSample reference**	**BET SSA (m^2/g) ± 2SD**
Quantachrome Instruments/NPL operator	ZB250#64#BET1 (scoop sampling)	At the beginning of the project	N/A	15.1 ± 0.6 (mean value of two replicates)
Meritics Ltd/MCA operator	NM111 ZnO Z-Cote HP1 (JRC spin riffled vials)	Towards the end of the project	0803	15.7 ± 0.04
			1951	15.5 ± 0.05
			1455	15.4 ± 0.05
			2017	15.5 ± 0.05
			2100	15.1 ± 0.05
			4414	15.3 ± 0.04

BASF powder samples – NM110 - Z-COTE ZnO, BASF Germany				
Operator/Instrument manufacturer	**Subsampling description/batch number**	**Relative time of analysis**	**Subsample reference**	**BET SSA (m^2/g) ± 2SD**
Quantachrome Instruments/NPL operator	ZC250#20#BET1 (scoop sampling)	At the beginning of the project	N/A	12.4 ± 0.6
Meritics Ltd/MCA operator	NM 110 ZnO Z-Cote (JRC spin riffled vials)	Towards the end of the project	0979	11.9 ± 0.01
			0599	12.1 ± 0.01
			0945	12.0 ± 0.01
			4779	11.9 ± 0.01
			4410	11.9 ± 0.01
			3911	11.9 ± 0.01

Results in Table 21 indicate that there is little difference in the BET value between the spin riffled *vs.* scoop sampling method. Interestingly, results also show little difference as to sample quality when analysed in the beginning *vs.* end of the PROSPEcT project and that results are independent on either the operator or manufacturer of the instrument used. Although this seems to indicate that there is little difference between spin riffled versus scoop sampling methods, this is only true in as much as what can be detected by the BET technique. Subsequently, this will be governed the instrument's detection limit. In addition, the corresponding particle size information should ideally complement the BET dataset above.

2 HOMOGENEITY TESTING FOR JRC POWDERS (AS SUBSAMPLED USING A SPINNING RIFFLER)

This sub-task under the PROSPEcT project was conducted in relation to the potential of using the PROSPEcT powders as potential future reference material. The role of NPL here is to act as a participating laboratory in this homogeneity study, led by JRC. The guidelines given to us by JRC include:

a) The choice of techniques chosen for this study i.e. SEM, XPS and BET.
b) The statistics associated required ie. how many replicates per vial to study and how many vials per nanomaterial type in total. This study performed measurements on 6 vials per particle type and with 3 replicates per vial, to be subsampled separately.
c) The need to open vials for analysis under inert argon environment.

Only two out of the seven PROSPEcT powder types were analysed for homogeneity: BASF's Z-COTE and Z-COTE HP1.

All analysis for this study was conducted in-house except for the BET measurements, which were outsourced to MCA Services, UK.

The output of this study is shown in Table 22, Table 23 and Table 24 below, which correspond to the SEM, XPS and BET results. Results were sent to JRC via NIA for further data processing. Further details on the study can be found on the NAPIRA hub database.

Table 22. SEM homogeneity test results, displaying primary particle size values (and corresponding mean Feret's diameter) for BASF: Z-COTE and Z-COTE-HP1 spin riffled samples.

CHARACTERISATION- NM 111 – ZINC OXIDE – Z-COTE HP1; 2 g (+/-) 10 mg				
Batch number on JRC vials	**Replicate number**	**Mean Feret diameter (nm)**	**s.d.**	**Number of particles analysed**
0830	rep1	92.4	59.5	144
	rep2	82.0	52.6	206
	rep3	66.8	48.8	189
1951	rep1	89.6	70.2	177
	rep2	73.6	60.1	222
	rep3	70.0	57.1	193
1455	rep1	92.9	54.5	178
	rep2	86.3	66.6	221
	rep3	99.5	72.3	258
2017	rep1	81.1	59.3	214
	rep2	72.7	53.0	219
	rep3	76.5	57.2	212
2100	rep1	78.1	64.8	224
	rep2	73.7	56.4	228
	rep3	88.7	63.6	186
4414	rep1	73.6	71.4	226
	rep2	68.2	53.7	232
	rep3	73.7	51.1	221

CHARACTERISATION- NM110 – ZINC OXIDE Z-COTE; 2 g (+/-) 10 mg				
Batch number on JRC vials	**Replicate number**	**Mean Feret diameter (nm)**	**s.d.**	**Number of particles analysed**
0979	rep1	110.8	73.9	163
	rep2	113.6	69.7	184
	rep3	102.3	60.4	190
0599	rep1	87.7	56.0	192
	rep2	94.0	72.8	239
	rep3	89.2	70.2	236
0945	rep1	98.3	60.6	209
	rep2	103.2	63.3	166
	rep3	107.7	67.4	156
4779	rep1	99.5	62.6	178
	rep2	111.1	74.3	174
	rep3	110.8	70.8	174
4410	rep1	99.5	56.5	209
	rep2	106.2	68.5	201
	rep3	104.5	64.0	214
3911	rep1	109.4	70.4	213
	rep2	113.9	68.4	209
	rep3	108.9	62.3	178

Table 23. XPS homogeneity test results, displaying element atomic concentrations. The powders were prepared as pellets for the purpose of the analysis, for BASF: Z-COTE and Z-COTE-HP1 spin riffled samples.

CHARACTERISATION- NM 111 – ZINC OXIDE – Z-COTE HP1 ; 2 g (+/-) 10 mg					
Batch number on JRC vials	**Replicate number**	**C 1s %**	**O 1s %**	**Si 2s %**	**Zn 2p3/2 %**
0803	rep1	21.5	44.0	1.8	32.6
		21.9	43.8	1.9	32.4
	rep2	24.8	41.5	2.0	31.8
		25.5	41.3	1.5	31.7
	rep3	25.5	41.3	1.5	31.6
		25.9	40.7	1.9	31.5
1951	rep1	31.2	37.1	1.4	30.3
	rep2	29.2	39.0	1.7	30.1
	rep3	29.9	38.5	2.0	29.7
1455	rep1	31.5	37.2	1.6	29.7
	rep2	30.5	38.1	1.1	30.3
	rep3	32.0	36.9	1.4	29.6
2017	rep1	29.6	38.6	1.8	30.0
	rep2	30.1	38.0	1.6	30.3
	rep3	30.4	37.8	2.2	29.6
2100	rep1	30.3	37.6	1.6	30.5
	rep2	31.8	36.6	1.8	29.7
	rep3	31.5	37.0	1.2	30.3
		30.0	37.9	1.6	30.5
4414	rep1	31.1	37.6	1.2	30.1
		31.7	36.9	1.6	29.8
	rep2	28.2	39.4	2.0	30.5
		29.0	38.9	1.9	30.1
	rep3	29.2	38.4	2.2	30.2

CHARACTERISATION- NM110 – ZINC OXIDE Z-COTE 2 g (+/-) 10 mg					
Batch number on JRC vials	**Replicate number**	**C 1s %**	**O 1s %**	**Si 2s %**	**Zn 2p3/2 %**
0979	rep1	24.2	39.3	0.0	36.5
	rep2	24.8	39.6	0.0	35.6
	rep3	25.9	39.2	0.0	34.8
0599	rep1	24.1	40.2	0.0	35.7
	rep2	26.2	39.1	0.0	34.7
	rep3	26.6	39.0	0.0	34.4
0945	rep1	23.7	40.3	0.0	36.0
	rep2	25.0	39.6	0.0	35.5
	rep3	25.9	39.4	0.0	34.7
4779	rep1	23.2	26.0	0.0	36.2
	rep2	26.0	39.3	0.0	34.7
	rep3	25.6	39.6	0.0	34.7
4410	rep1	19.6	41.2	0.0	39.2
	rep2	22.2	40.2	0.0	37.6
	rep3	22.0	40.7	0.0	37.3
3911	rep1	20.3	40.8	0.0	38.9
	rep2	21.5	40.3	0.0	38.2
	rep3	22.8	40.2	0.0	36.9

Table 24. BET homogeneity test results, displaying the specific surface area values, for BASF: Z-COTE and Z-COTE-HP1 spin riffled samples. Errors indicate ± 1 SD.

CHARACTERISATION- NM 111 – ZINC OXIDE – Z-COTE HP1 ; 2 g (+/-) 10 mg		
Batch number on JRC vials	**Replicate number**	**BET SSA (m^2/g)**
0830	rep1	15.7 ± 0.0483
	rep2	15.7 ± 0.0413
	rep3	15.8 ± 0.0443
1951	rep1	15.5 ± 0.0466
	rep2	15.5 ± 0.0437
	rep3	15.5 ± 0.0472
1455	rep1	15.5 ± 0.0462
	rep2	15.4 ± 0.0415
	rep3	15.4 ± 0.0493
2017	rep1	15.5 ± 0.0479
	rep2	15.4 ± 0.0454
	rep3	15.4 ± 0.0479
2100	rep1	15.1 ± 0.0485
	rep2	15.1 ± 0.0437
	rep3	15.1 ± 0.0428
4414	rep1	15.3 ± 0.0467
	rep2	15.2 ± 0.0459
	rep3	15.3 ± 0.0414

CHARACTERISATION- NM110 – ZINC OXIDE Z-COTE 2 g (+/-) 10 mg		
Batch number on JRC vials	**Replicate number**	**BET SSA (m^2/g) ± 1SD**
0979	rep1	11.9 ± 0.0102
	rep2	11.9 ± 0.0075
	rep3	11.9 ± 0.0083
0599	rep1	12.1 ± 0.0062
	rep2	12.1 ± 0.0121
	rep3	12.0 ± 0.0107
0945	rep1	12.0 ± 0.0079
	rep2	12.0 ± 0.0098
	rep3	12.0 ± 0.0087
4779	rep1	11.9 ± 0.0059
	rep2	12.0 ± 0.0043
	rep3	12.0 ± 0.0090
4410	rep1	11.9 ± 0.0094
	rep2	12.0 ± 0.0093
	rep3	11.9 ± 0.0085
3911	rep1	11.9 ± 0.0070
	rep2	11.9 ± 0.0039
	rep3	11.9 ± 0.0076

3. IMPURITIES IN THE SAMPLES

For these samples to be used as reference material, the purity of the materials needs to be within a level deemed acceptable for toxicity testing. During the process of our investigations, on dissolution properties (see section 2.2.1, Table 7 for further details) using ICP-MS, the test results seem to indicate a level of Zn impurity in the CeO_2 batches; this however did not occur the other way around i.e. no Ce impurity was found inside the ZnO batches. Table 25a and b show the levels of contaminants in the samples throughout the dissolution period (of ~ 20 days).

Table 25. The amount of background contamination of a) Zn in CeO2 samples and b) Ce in ZnO samples.
a)

Cerium Oxide sample	Ecotox media	Day of dispersion	Background Zn in the samples (ng/g)
Nanograin CeO2, Umicore Belgium	DI water	2	187
	Fish media	2	254
	Sea water	2	309
	Daphnia	2	619
	DI water	6	269
	Fish media	6	234
	Sea water	6	326
	Daphnia	6	449
	DI water	9	294
	Fish media	9	1049
	Sea water	9	554
	Daphnia	9	662
	DI water	14	41.5
	Fish media	14	711
	Sea water	14	581
	Daphnia	14	579
	DI water	21	364
	Fish media	21	822
	Sea water	21	630
	Daphnia	21	800
Micron CeO2, Sigma Aldrich, UK	DI water	2	Data missing
	Fish media	2	334
	Sea water	2	168
	Daphnia	2	401
	DI water	6	206
	Fish media	6	641
	Sea water	6	232
	Daphnia	6	583
	DI water	9	191
	Fish media	9	504
	Sea water	9	249
	Daphnia	9	498
	DI water	14	189
	Fish media	14	554
	Sea water	14	332
	Daphnia	14	414
	DI water	21	112

	Fish media	21	591
	Sea water	21	279
	Daphnia	21	471
Ceria Dry CeO2, Antaria, Australia	DI water	2	166
	Fish media	2	273
	Sea water	2	157
	Daphnia	2	378
	DI water	6	284
	Fish media	6	500
	Sea water	6	199
	Daphnia	6	310
	DI water	9	294
	Fish media	9	475
	Sea water	9	226
	Daphnia	9	360
	DI water	14	304
	Fish media	14	365
	Sea water	14	174
	Daphnia	14	308
	DI water	21	346
	Fish media	21	439
	Sea water	21	209
	Daphnia	21	372

b)

Zinc Oxide sample	**Ecotox media**	**Day of dispersion**	**Background Ce in the samples (ng/g)**
B. Nanosun ZnO, Micronisers, Australia	DI water	2	1.64
	Fish media	2	2.21
	Sea water	2	1.78
	Daphnia	2	1.45
	DI water	6	0.89
	Fish media	6	<0.2
	Sea water	6	0.41
	Daphnia	6	1.01
	DI water	9	1.36
	Fish media	9	1.36
	Sea water	9	2.64
	Daphnia	9	1.13
	DI water	14	1.54
	Fish media	14	1.90
	Sea water	14	2.69
	Daphnia	14	1.60
	DI water	21	0.99
	Fish media	21	1.15
	Sea water	21	4.18
	Daphnia	21	0.96
Micron ZnO, Sigma Aldrich	DI water	2	1.67
	Fish media	2	2.34
	Sea water	2	1.73
	Daphnia	2	1.82
	DI water	6	0.81
	Fish media	6	0.92

	Sea water	6	1.00
	Daphnia	6	1.20
	DI water	9	<0.2
	Fish media	9	<0.2
	Sea water	9	1.41
	Daphnia	9	1.11
	DI water	14	0.78
	Fish media	14	0.76
	Sea water	14	1.17
	Daphnia	14	0.97
	DI water	22	1.97
	Fish media	22	2.02
	Sea water	22	1.92
	Daphnia	22	2.02
Z-COTE ZnO, BASF	DI water	2	1.81
	Fish media	2	1.87
	Sea water	2	1.86
	Daphnia	2	1.61
	DI water	6	1.10
	Fish media	6	0.99
	Sea water	6	<0.2
	Daphnia	6	Data missing
	DI water	9	0.95
	Fish media	9	1.44
	Sea water	9	0.97
	Daphnia	9	1.10
	DI water	14	2.07
	Fish media	14	1.07
	Sea water	14	1.10
	Daphnia	14	1.43
	DI water	21	1.88
	Fish media	21	1.75
	Sea water	21	1.93
	Daphnia	21	1.75

In the case of PROSPEcT CeO_2 samples, the range of background Zn found in the samples varied between 41.5 ng/g (as in the case of Nanograin in DI water after 14 days of dispersion) to 1049 ng/g (Nanograin in fish medium after 9 days of dispersion). There seems to be no correlation on the level of contamination with respect to: sample type, type of media it is dissolved in, or the time after dispersion. In contrast, the amount of Ce impurity in the ZnO samples seems to be little, ranging from <0.2 to 4.18 ng/g.

In addition to results associated with dissolution testing, the XPS data also show impurity that exists with CeO_2 samples, however this was shown only for Micron CeO_2 from Sigma Aldrich, UK with an element atomic concentration of 0.2 % (refer to Table 7).

4 THE DEVELOPMENT OF NEW PLATFORMS AND TECHNOLOGIES FOR NANOMATERIAL CHARACTERISATION

During the testing of the PROSPEcT nanomaterials, it became clear that there are limitations associated with the current laboratory tools for the characterisation of these materials. Figure 9 below aims to identify where common laboratory techniques like DLS and SEM sit on a technology space map, in

which three important criteria have been identified sensitivity (x-axis), selectivity (y-axis) and *representativeness* (z-axis). Ideally, an instrument should have a high degree of sensitivity (to single particle level), high selectivity (to measure in the presence of potentially interfering substances in the ecotox media) and high *representativeness* (such that the data is a representation of the entire population rather than a small subset; this will subsequently contribute towards the accuracy and repeatability of the measurements). The ideal tool sits on vertex C. Research activities should aim to employ and subsequently validate the techniques that belong on vertex C. However, the ideal tool cannot be limited to the solely to these three criteria; other requirements have been identified, as summarised in the inset of Figure 9.

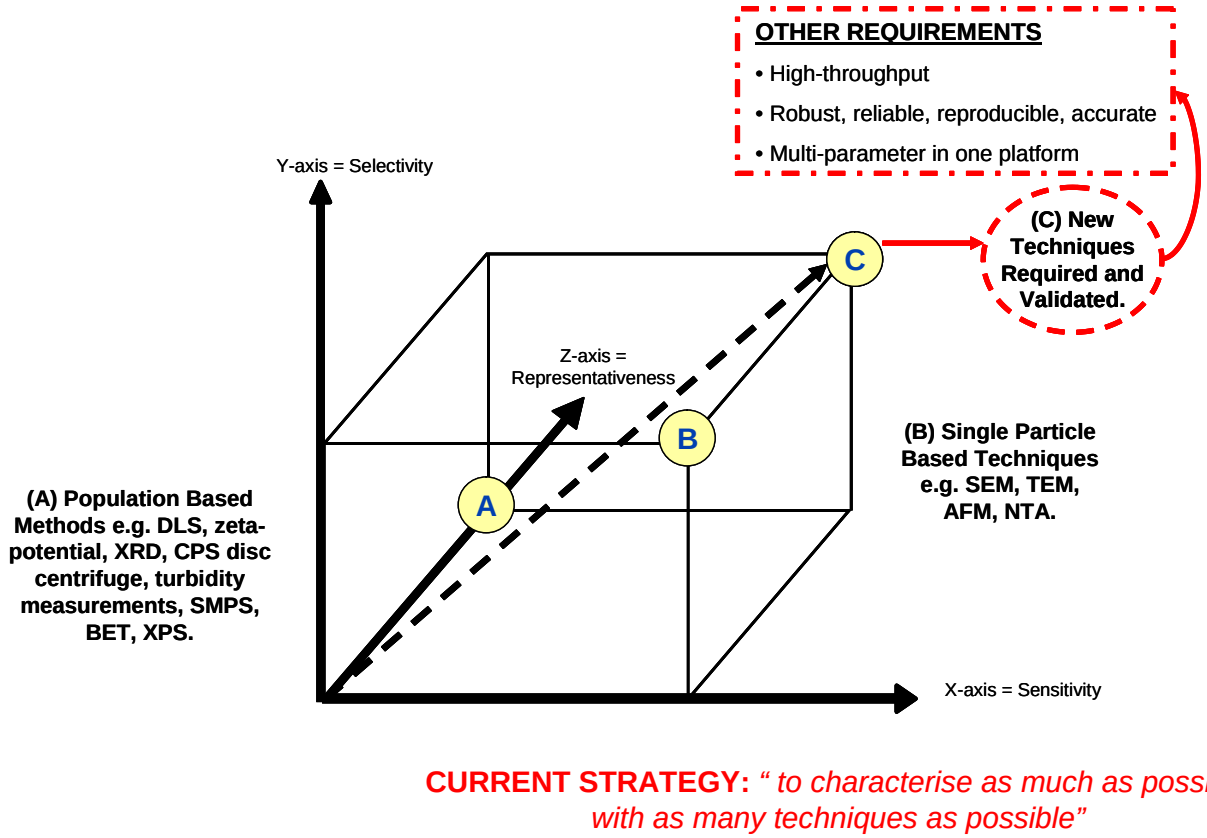

Figure 9. Technology space map: tools/techniques for nanoparticle characterisation in complex environmental media assessed against three identified (amongst others) criteria of: sensitivity (x-axis), selectivity (y-axis) and "representativeness" (z-axis).

Part of our research activity has been in the development of new/existing technologies for the characterisation of nanomaterials. Our progress to date will be discussed in this sub-section.

4.1 The development of a prototype UV/ozone cleaning technique

The purpose of developing this platform was to improve the selectivity for nanomaterial characterisation by using UV/ozone (O_3) cleaning technology in order to remove surface and background carbon contamination. A prototype system was developed and tested; preliminary results, as detailed elsewhere in published report (NIA website) indicated that the prototype here was shown to be unfit for purpose.

4.2 The development of TOF-SIMS for surface chemistry and depth profiling of nanomaterials

The purpose of developing this platform was not only to probe the chemical surface composition of the surface (sensitive to the topmost 1-2 nm of the surface), but to conduct depth profiling. Initial preliminary studies, as reported in the Interim report had shown some of the hurdles, which would need to be overcome prior to adopting this technology for nanomaterial characterisation:

a) The potential of nanomaterial damage (this was shown to be the case for gold nanoparticles). This necessitates low energy ion beams, very low doses and sample cooling to prevent melting during compositional depth profiling.
b) The need to have better surface coverage or alternative sample mounting e.g. close packed structure, to distinguish nanomaterial signals from those of the substrate (background); this would be crucial to the successful analysis of nanomaterials in TOF-SIMS. Currently, work at NPL is still ongoing on this front.
c) The need for modelling, for the purpose of validating the reliability of the data collected. Work had started in this respect and the reader is asked to refer to a recent NPL publication that describes the topography effect and monoatomic ion sputtering of large nanoparticles (6).

Although this technology and its applications for depth profiling of nanomaterials is still at its infancy, we have attempted to employ TOF-SIMS to elucidate surface chemistry of the PROSPEcT powders. Our findings had shown that for the purpose of evaluating sample purity and type of contaminants present, the XPS technique provides a more informative and quantitative chemical analysis. The main challenge here has been related to restrictions imposed by sample mounting requirements; the full report can be found in NAPIRA database.

4.3 The development of microfluidic capillary electrophoresis with conductivity detection for nanomaterial characterisation

The purpose of developing this platform is to have a high-throughput platform for monitoring the kinetics of ZnO dissolution. The drive here is to have a platform capable of incorporating two functions:

a) To separate the ions from the solid particles in the aqueous suspension.
b) The ability to detect ion concentration quantitatively.

The current method, of supernatant extraction followed by ICP-MS analysis used in the PROSPEcT project, is not only laborious/time-consuming and expensive but potentially can lead to unreliable results (mainly in the extraction step of the supernatant i.e. the removal of the nanomaterial to ensure that it is absent in the sample prior to ICP-MS analysis, which is highly operator dependent). This work began in January 2012 and we are at a stage in which the microfluidic platform has been set up at NPL and tested for reference ions Li+, Na+ and K+. We will continue with this work, to test the system's feasibility to measure zinc ion dissolution; this work will continue until August 2012 (due to an extension granted by NMO and DEFRA and the additional fund of £7715 provided by DEFRA). This work will be continued in collaboration with the University of Exeter, who will be aiding us to show its potential for use with real ecotox media.

4.4 Novel use of the condensation particle counter.

The aim of this project was a further proof of concept for the extended use of a Condensation Particle Counter for nanomaterial characterisation. This technique can potentially allow material-dependent nanoparticle characterisation. The PROSPEcT funding was used to:

a) further developed the Condensation Particle Counter for its novel use in nanomaterial characterisation.
b) modify the method to not only yield particle number concentration but to enable the differentiation of the different material types of particles detected (based on the material's affinity for butanol).
c) further modify the method to improve the platform's capability by extending the range of particle sizes being differentiated and hence resulting in a 2-D plot (where the particle number concentration has been shown to be dependent on both the internal temperatures within the CPC and particle size). The platform has previously been shown to work with 20 nm particles (soot, sodium chloride, ammonium nitrate).
d) test the platform for ZnO PROSPEcT powder, where data are currently awaiting further analysis.

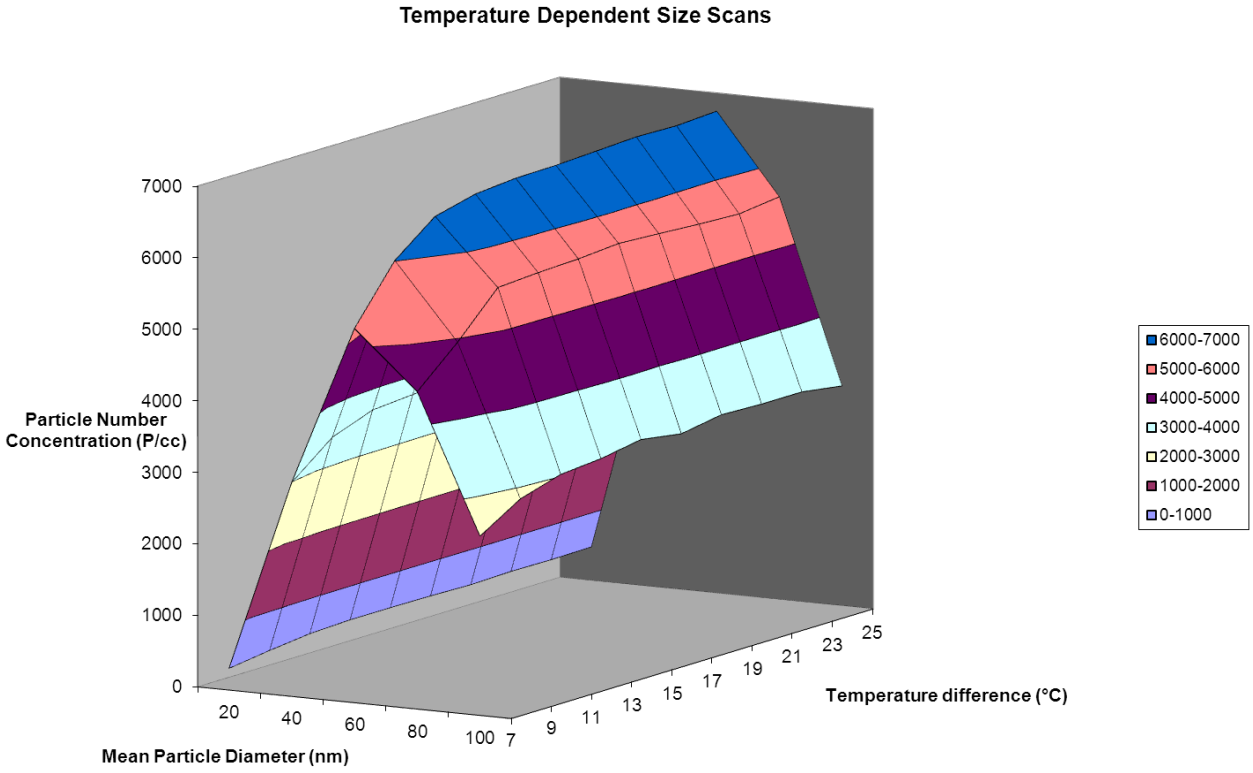

Figure 10: Temperature dependent CPC scans.

Our findings have shown that the technique has potential to perform near to real time detection and to discriminate different nanoparticle type. It is however without limitations in that the nanomaterials must have: a) a high concentration above background b) a sufficiently different surface chemistry c) concentrations that needs to have a reasonable stability over periods in the order of 5 minutes.

APPENDIX 3: DETAILS OF MEASURANDS AND MEASUREMENT TECHNIQUES USED

Table 26. Parameters, Corresponding Measurand and potential techniques for measurement.

Parameter	Definition	Measurand	Main techniques identified as suitable for the provision of OECD physicochemical endpoints
Aggregation/ Agglomeration	Aggregate is the assembly of particles rigidly joined together as by partial fusion, sintering or by growing together; this may result in the external surface area to be significantly smaller than the sum of calculated surface areas of the individual components. Agglomerate is an assembly of particles that are loosely attached. (ISO 14887)	For "as received" powders this will be a qualitative assessment to reflect the extent of aggregation/agglomeration. The effect of external influences (e.g. addition of salt in the liquid medium) on aggregation/agglomeration rate can be monitored indirectly through turbidity measurements and their evolvement through time.	High resolution SEM for the qualitative assessment of the "as received" powders, turbidity meter for dispersion and the effects of different liquid media composition on the aggregation/agglomeration rate.
Dispersion stability	This is the tendency for the dispersion to remain in its current physical and chemical state.	This will be: a) half-life (time it takes for particle concentration to decrease by half) b) zeta-potential	Turbidity meter Doppler microelectrophoresis
Dissolution	This refers to the mass proportion of the nanomaterial in colloidal suspension that has lost its particulate character i.e. from a particle form to ionic or molecular form.	Ion concentration over a specific period of time.	This involves sample extraction i.e. the removal of the particulate form from the ionic form. Subsequent analysis of ion concentration will be made with ICP-MS.
Crystallite size	This is the size of a single crystal inside a particle or a grain.	XRD diffraction with analysis using the Scherrer equation.	XRD

Crystalline phase	This will describe the crystalline structure.	Crystalline phase description (ie.lamellar, hexagonal or cubic structures) acquired through spectral matching search in a central database.	XRD
Particle size and particle size distribution	Dimensions of particles as determined by specified measurement conditions and with a specified method eg. CPS disc will yield particle size by weight.	Mean particle size (as described by the Feret diameter), particle size distribution and oversize or undersize percentiles values (i.e. D10, D50 and D90 values) from the distribution. For example, for oversize D10 = 187 nm as reported by the CPS disc centrifuge will mean that 10% of the mass has a particle diameter larger than 187 nm.	SEM, TEM, CPS disc centrifuge, SMPS.
Surface area (and porosity) using BET	Area of exposed particle (although the measured specific area may not necessarily mean the surface area that is biologically available).	BET surface area per unit mass	BET
Zeta-potential	This characterises the electric properties of solid surface in contact with liquid. Its value is related to dispersion stability.	Electrophoretic mobility measurement and subsequent estimation through the use of the Smoluchowski equation.	Doppler Microelectrophoresis
Surface chemistry	Chemical composition of the outermost layers. The precise definition of "the surface" depends on the information depth of the techniques. XPS has an information depth up to 10 nm and TOF-SIMS is sensitive to the topmost 1-2 nm of the surface. In addition to surface chemistry, composition as a function of depth may be obtained using sputter depth profiling in TOF-SIMS.	Elemental species (e.g. atom% of each element), chemical bonding (e.g. % of C=O, C–O bonds), and detection and identification of chemical species (e.g. organic molecules) on surfaces.	XPS (potentially TOF-SIMS)

Redox Potential	Redox potential is an electrical measurement of how readily a system will donate (reduce) or accept electrons (oxidise).	This is a measure of its affinity for electrons compared with hydrogen, measured in volts and thus corresponds to the potential range of predominant redox reactions under given conditions. Reliable measurement requires that equilibrium is established not only at the electrode but also among various redox couples in solution.	This is an electrical measurement (potential difference between a Pt vs Ag/AgCl electrode) that show the tendency of a medium to transfer electrons to or from an inert electrode, as measured by an ORP (oxygen-reduction potential) electrode.
Radical formation under photocatalytic conditions	The photocatalytic activity of materials refers to their ability to create electron-hole pairs under light irradiation, which then generate reactive oxygen species (ROS) such as free radicals (e.g. superoxide radicals, hydroxyl radicals, etc.), hydrogen peroxide, singlet oxygen, etc.	ROS lifetime is generally below the millisecond range, which makes their detection challenging. One strategy to detect ROS formation is to use scavenging substances that get oxidised by ROS into stable chemical compound whose concentration can be detected. A method for assessing the general oxidative activity of the NMs under irradiation is by using potassium iodide (KI) test. The oxidation of iodide ions results in the production of tri-iodide ions, whose concentration can be assessed by measuring optical absorbance at 352 nm.	UV-vis spectroscopy for the detection of tri-iodide ions.
Dustiness	The dustiness of a material is the mass of dust generated per mass of material under testing.	Dustiness index is a means of determining the relative values that represent the amount of dust produced when the powder is handled in a standard manner.	As measured by a rotating drum dustiness tester. Eurononon EN15051 gravimetric measurement 35 ml of dust.
Representative TEM images	Images of the particles with subnanometer resolution.	TEM micrographs for the analysis of primary particle size/ size distribution.	TEM

Pour density	The pour density (or bulk density) is the apparent density of a bed of material formed in a container of standard dimensions when a specified amount of the material is introduced without settling. The 'tap density' is the density after the material has been subsequently vibrated or tapped under standard conditions.	Bulk density, tapped density and the Carr index	Copley JV 2000
Porosity	Volume of pores per mass.	The Barrett-Joyner-Halenda (BJH) method was used to determine the porosity	BET

Table 27. Main techniques for the measurement of OECD physico-chemical endpoints and the corresponding protocols.

Technique	Protocol
High Resolution SEM	SEM images were obtained using a Supra 40 field emission scanning electron microscope from Carl Zeiss (Welwyn Garden City, Hertfordshire, UK), in which the optimal spatial resolution of the microscope was 1.2 nm. The in-lens detector images was used to obtain the images, an accelerating voltage of 15 kV, a working distance of ≈ 3 mm, and a tilt angle 0° was used. The SEM was calibrated using a SIRA grid calibration set (SIRA, Chislehurst, Kent, UK). These are metal replicas of cross ruled gratings of area of 60 mm^2 with 19.7 lines/mm for low magnification and 2160 lines/mm for high magnification calibrations, accurate to 0.2 %. For analysis of the "as received" nanoparticle powder, a sample of the powder was sprinkled over a SEM carbon adhesive disc; one side of the carbon disc was placed securely on a metal stub, whilst the other side was exposed to the nanoparticle powder. Excess powder was removed by gently tapping the stub on its side until a light coating of powder on the surface became apparent. For analysis of nanoparticles dispersed in liquid media, sample preparation required the nanoparticles to be "fixed" on to a substrate surface. This involved the deposition of an appropriate liquid sample (1 ml) on to a poly-l-lysine coated microscope glass slide (purchased from Fisher Scientific, UK) and allowing it to incubate for a period of 5 min at room temperature (≈ 20 °C) before dipping in a beaker of water in order to remove unbound nanoparticles. Slides were then allowed to dry under ambient conditions for ≈ 2 h before they were thinly sputtered with gold using an Edwards S150B sputter coater unit (BOC Edwards, UK). Sputtering was conducted under vacuum (≈ 7 mbar or 0.7 mPa), while passing pure, dry argon into the coating chamber. Typical plate voltage and current were 1200 V and 15 mA, respectively. The sputtering time was approximately 10 s, which resulted in an estimated gold thickness of no more than 2 nanometres being deposited on top of the substrate. An adequate magnification was chosen for image acquisition e.g. for the estimation of primary particle mean diameter. The shape and limits of the primary particles should become apparent.
TEM	Sample preparation was carried out by putting a small amount of the nanomaterial (10 mg) into a clean glass container and then dispersing in 3 ml of ethanol. The particles were deposited on TEM grids and images acquired using a Hitachi 2300A instrument operated at 200 kV. The instrument is based at the University of Surrey, Guildford and analysis was carried out by NPL personnel. An adequate magnification (in which the shape and limits of the primary particles should become apparent) was chosen for image acquisition and images were subsequently analysis for the estimation of primary particle size/size distribution profiles.

Image analysis from SEM and TEM micrographs	Initially, SEM micrographs were analysed by manually tracing contours of primary particles on to a transparency sheet. The transparency sheet was scanned for further image analysis using ImageJ software, which automatically calculated particle diameter dimensions. This manual tracing on transparency sheet was found to be time consuming and laborious. This method of tracing was replaced by the use of a tablet PC and a digital pen; this allows outlining the contours of particles directly and with ease and was shown to reduce the many laborious hours spent using the transparency sheet. This was carried out for the analysis of SEM micrographs for the purpose of homogeneity testing and for the TEM analysis.
Turbidity measurements	Turbidity was measured using HF Scientific – Micro100 RI turbidity meter (Cole-Palmer, UK); this meter has an infrared light source that meets the international standard ISO 7027 for turbidity measurements. The meter was calibrated on standards which are based on AMCO-AEPA-1 microspheres; these standards are traceable to standard formazin suspension. Standard values of 1000, 10 and 0.02 NTU were used to calibrate the meter. Prior to use, the meter was allowed to warm up for 30 minutes. Sample cuvettes (HF Scientific (USA)) were used to hold the sample. Note that glass thickness may vary between cuvettes, and also within the same cuvette. Hence, individual vials were indexed by finding the point of the cuvette in which light passes through to give the lowest reading; once indexed the holder was marked accordingly. Prior to their use, cuvettes were cleaned, in accordance to manufacturer's instructions. This involved washing the interior and exterior of the cuvette with a detergent (2% Hellmanex in DI water); it was then rinsed several times in distilled water before finally rinsing in DI water. The cuvette was further rinsed with the sample two times before filling (30ml) and analysed. The cuvette was placed into the meter and signal allowed to settle before taking readings.
Zeta-potential	Electrophoretic measurements were obtained using a Zetasizer Nano ZS (Malvern Instruments, UK) equipped with a 633 nm wavelength laser. The reference standard (DTS1230, zeta-potential standard from Malvern) was used to qualify the performance of the instrument. Sample preparation involved the filling of a disposable capillary cell (DTS1060, Malvern). Prior to their use, these cells were thoroughly cleaned with ethanol and de-ionised water, as recommended by the instrument vendor. For analysis, the individual cell was filled with the appropriate sample and flushed before re-filling; measurements were carried out on the second filling. Malvern Instrument's Dispersion Technology software (Version 4.0) was used for data analysis, and zeta-potential values were estimated from the measured electrophoretic mobility data using the Smoluchowski equation.

<table>
<tr><td>Extraction of supernatant in a colloidal suspension</td><td>This is the removal of solid nanomaterial in the dispersion prior to sample analysis using ICP-MS; this is to ensure that the sample was left with the ionic form. The particle extraction involved three main steps. Firstly, the extraction of particles using filtration, which was carried out using Millipore Express PES membrane, 0.1 µm pore size filter (Fisher, UK) under vacuum. The second step involved taking the resultant filtrant and transferring to an appropriate centrifugation vial. The vial containing the sample was centrifuged (Centrifuge 5430, Eppendorf, UK) (7500 rpm for one hour) resulting in the formation of a pellet at the bottom of the vial. Lastly, the resultant clear supernatant was extracted using a Peri-Star Pro peristaltic pump (World Precision Instruments, UK); this was done carefully, so as to not disturb the pellet. Only half of the supernatant was collected, stored in the freezer for further analysis using ICP-MS.</td></tr>
<tr><td>ICP-MS for measurement of the extracted supernatant, outsourced to LGC</td><td>The analysis of the supernatant was subcontracted and performed by personnel at LGC (Laboratory Government Chemist, UK). The ICP-MS analysis was carried out using an Agilent 7500ce ICP-MS Octopole Reaction System, operating in standard (no collision cell gas) mode for Cerium (Ce) and Helium mode for Zinc (Zn). The instrument is UKAS accredited and was set up following standard operating procedure (SOP) INS/A1-0013. The samples were equilibrated at room temperature, then agitated, to ensure homogeneity. An aliquot of 0.2g – 0.23g was taken from each sample and digested in a CEM Discover microwave, SOP INS/A1-0014, using a mixture of HNO_3/H_2O_2. All samples were digested and analysed over a period of 5 days. Validation was carried out following SOP INS/A1-0015, this includes spiked recoveries and replicate analyses. The limit of detection (LoD) and limit of quantitation (LoQ) are given in the table below. The estimated uncertainty at 95% confidence (k=2) is 12% for Zn and 20% for Ce. Results below the LoQ are likely to have a higher error.
<table>
<tr><td colspan="3">Limit of detection (LoD) and Limit of quantification (LoQ) for Zn and Ce</td></tr>
<tr><td></td><td>Zn concentration (ng g^{-1})</td><td>Ce concentration (ng g^{-1})</td></tr>
<tr><td>LoD</td><td>5</td><td>0.2</td></tr>
<tr><td>LoQ</td><td>15</td><td>0.8</td></tr>
</table>
</td></tr>
</table>

XRD	X-ray diffraction traces were obtained using a Siemens D5000 diffractometer. This consisted of a theta-theta goniometer and an NPL specimen stage. The X-ray source used for these measurements was the Cu-Kα X-ray (40 kV, 30 mA), a Ni filter was used to remove the Cu-Kβ component of the X-ray. The X-ray optics consisted of a 0.6mm anti scatter slit, a 1mm collimation slit and a 1mm detector slit. The diffraction measurement was conducted using coupled theta-theta drives in standard Bragg-Brentano geometry. The data was collected over a 2-theta range of 5° to 150° using a step size of 0.010° and a count time of 1.5 s/step. The diffracted data was electronically collected and stored on the laboratory PC. Prior to the measurement, the X-ray beam was aligned by placing the X-ray source and the detector in line and passing the X-ray beam through a glass slit, the direct beam was attenuated using copper foil placed in front of the detector. Having aligned the two drives and the stage height a standard reference material (corundum) was used to check the alignment over a range of 2-theta values. Having collected the full diffraction trace the Scherrer equation was used to evaluate the crystallite size. The data was outsourced to Southampton Chemistry Analytical Solutions (SCAS), for further interpretation of the diffraction datasets required for the extraction of crystalline phase information. Data analysis was performed using a computer program EVA 16.0 (Copyright © Bruker-AXS 1996-2010). The pattern matches were performed using this software linked to the ICDD (International Centre for Diffraction Data) PDF (Powder Diffraction File) database 2005; these database entries are experimentally measured data that have been extracted from the literature.
CPS disc centrifuge	Particle size distribution by centrifugal sedimentation was acquired using CPS Disc Centrifuge Model DC 20000 instrument (Analytik Ltd, UK). At the start of the method, the centrifuge was brought up to speed by partially filling the disc with a sucrose gradient fluid and dodecane cap fluid. The purpose of the gradient fluid was to stabilise the sedimentation; the purpose of the cap fluid was to maintain the gradient inside the disc. The disc centrifuge was then allowed to equilibrate at 6000 rpm for 1 hour; this stable gradient was used within the following 6 hours. 0.2 ml of the nanoparticle sample (50 mg/L) was injected into the disc; a calibration standard was injected after every three samples. Analysis was run against a calibration standard, NIST traceable standard, PVC 0.377 micron. The Disc Centrifuge Control System software (CPS Instruments Inc.) was used to acquire and process the data.

SMPS	The NANEUM PA100 was used to produce an aerosol from the dry powder sample. After introduction of the NM into the PA100, the aerosol generated was passed through a stabilisation chamber. A Scanning Mobility Particle Sizer - SMPS (TSI 3080 SMPS), consisting of a DMA and CPC system, was used to determine the particle size distribution. The Differential Mobility Analyser (DMA) within the SMPS was calibrated using reference material polystyrene latex beads from NIST. The Condensation Particle Counters (CPC) within the SMPS setup was calibrated according to NPL's UKAS accredited (ISO 17025) procedure, using an internally calibrated Faraday Cup Electrometer and soot generator (model CAST 2). The SMPS was set to record at 4-minute intervals in parallel with a CPC. The data was processed using TSI Aerosol Instrument Management (AIM) software. The particle concentration from the CPC (TSI 3022a) was used to correct the size distribution gained from the SMPS by removing the effects of any fluctuations or trends within the particle source. The size distribution was also analysed using an in-house curve-fitting program (as implemented in a recent SMPS intercomparison at METAS).
BET for specific surface area	BET surface area measurements were determined using Autosorb-1 (Quantachrome Instruments). The Autosorb-1 was calibrated using a quartz rod of a known volume, which is traceable to NIST. This calibration was then further checked using two BAM certified reference materials: BAM-PM-102 (nominal SSA 5.41m^2g^{-1}) and BAM-PM-104 (nominal SSA 79.8 m^2g^{-1}). These two reference materials allowed the range of SSA of the nanoparticles to be encompassed with known specific surface area materials, thus adding confidence to the measurements. Surface area measurements were acquired using an 11-point BET gas adsorption method, with nitrogen as the adsorbate. Prior to analysis, the powdered sample was transferred to a sample bulb, then sealed and subsequently de-gassed overnight at 300°C under a high vacuum and subsequently weighed on a analytical balance in order to determine the sample mass after the degassing step.

BET SSA and Porosity, outsourced to MCA Services	Micromeritics TriStar II (3020) was used for the collection of nitrogen adsorption/desorption isotherm data up to a saturation pressure of approximately 0.995 P/Po. The analysis was typically conducted to measure 45 adsorption relative pressure points and 23 desorption relative pressure points. Samples were outgassed overnight in vacuum at 300 ºC using a Micromeritics VacPrep apparatus prior to analysis. In order to indicate any possible microporous nature of the materials additional relative pressure data were also collected at pressures lower than the usual starting point for analysis using this instrument. These were in the approximate range 0.005 to 0.01 P/Po. The sample tube dead space was measured for each analysis using helium (CP grade) thus providing warm and cold freespace values. The same equipment, with the application of the same freespace measurement technique, was used with samples requiring **only** BET surface area analysis (i.e. the JRC homogeneity measurements). BET surface area was calculated using partial pressures in the nominal range 0.07 to 0.25. Data Reduction The pore size distribution is presented as pore size by volume and area from the adsorption isotherm using the BJH method. The lower limit of BJH calculations in terms of pore size (by diameter) is extended below the typical value in order to highlight any possible microporous nature of the materials. The pore size distribution data presented in the BJH reports is applied to a maximum of 1000Å, although data below approximately 20Å and should be considered only as a guide to the full porous nature of the materials. The total pore volume of the materials is calculated from the volume of nitrogen adsorbed at the maximum relative pressure obtained on the adsorption branch of the isotherm. Whilst the data reduction methods available are unsuitable for application to the micropore range, the characteristic shape of the adsorption isotherm at these low partial pressures would provide a good indication of the presence of micropores in the sample material.

XPS	XPS measurements were obtained in ultra high vacuum using a Kratos AXIS Ultra DLD (Kratos Analytical, UK) instrument fitted with a monochromated Al Kαsource, which was operated at 15kV and 5mA emission. Photoelectrons from the top few nanometres of the surface were detected in the normal emission direction over an analysis area of approximately 700 x 300 micrometres. Spectra in the range 1400 to –10 eV binding energy and a step size of 1 eV, using a pass energy of 160 eV were acquired from selected areas of each sample. The peak areas were measured after removal of a Tougaard background. The manufacturer's intensity calibration and commonly employed sensitivity factors were used to determine the concentration of the elements present. High-resolution narrow scans of some peaks of interest were acquired with a step size of 0.1 eV and 20 eV pass energy; the manufacturer calibrated the intensity calibration over the energy range. The energy scale was calibrated according to ISO 15472 Surface chemical analysis – X-ray photoelectron spectrometers – Calibration of energy scales. However, the charge neutraliser was used when acquiring the spectra, which shifted the peaks, by several eV. The C 1s hydrocarbon peak (285 eV binding energy) was used to determine the shift for identifying the peaks. Initially, the samples were prepared using carbon adhesive tape, which was used to affix the nanomaterials. As detailed in the Interim report, care was taken to cover the tape with the powders as completely as possible but some samples had better coverage than others and in a lot of cases signal from the tape was detected (contributing towards the carbon, oxygen and silicon signals) as well as the powder itself. Clearly this was not acceptable and our sample preparation protocol was further developed. Instead of sprinkling on carbon tape, pellets made from the powders were used instead. Pellets from the sample powders were produced using the KBr Quick Press pellet presser. The powder was loaded into the presser (½ to ¾ full) and then pressed to produce the pellets. The pellet presser was sufficiently cleaned in between sample preparations in order to avoid cross contaminations; this was done by washing the presser sufficiently with DI water, detergent and isopropanol.

Redox Potential by oxygen-reduction potential (ORP) electrode	Note: The original protocol associated redox potential (as detailed in the Interim Report) with the making of pellets for the electrode and subsequently measuring the redox potential via acquiring the cyclic voltamogram has been replaced by the following protocol: Dispersion of the individual nanomaterial in the appropriate liquid media was carried out in accordance with the protocol recommended under the PROSPEcT programme. Redox potential of the dispersions were measured using an ORP Oakton® Waterproof ORP Testr®, purchased from Cole Palmer UK. This measures the potential difference across two electrodes: a Pt electrode against a double junction Ag/AgCl reference electrode. The electrode was used according to the manufacturer's instructions. Prior to use the electrode was pre-conditioned in clean tap water for 30 minutes before rinsing in distilled water. When making measurements, the electrode was carefully placed in a vial containing the sample; with sufficient liquid sample to cover the sensing element. The electrode was carefully stirred a little and then placed in a fixed position, slightly above the bottom of the container. The signal output was allowed to settle for 5 minutes before a reading was taken and the "field potential" noted. After measurement, the electrode was cleaned with tap water and final rinse was with distilled water, after which further measurements could be made. When not in use, the electrode was stored in a solution of Oakton® electrode storage solution. The redox potential ORP electrode was calibrated against YSI® Zobell ORP Calibration Solution (purchased from Cole Palmer). This reagent was made available in dry form, and was reconstituted with 125 mL of DI water prior to use, after which the solution has ~ 6 months expiry date. This standard solution was also used to verify the performance of the electrode in the beginning and end of the study. For Ag/AgCl reference, the redox potential value for Zobell solution was 231 ±10 mV (depending on temperature); at ~ 20 C, this value was ~ 237 mV. Redox potential was carried out on freshly dispersed nanomaterial suspensions in various media i.e. DI water and four ecotox media (fish, daphnia, water flea and seawater). All field potential values recorded were subjected to an additive correction factor of +206 mV; this was necessary so that the final value was reported as if the reference electrode was a standard hydrogen reference electrode instead of the Ag/AgCl.

KI test under irradiated conditions	A 5 M KI (Sigma, St. Louis, MO) solution in ultra-pure water was freshly prepared; shaking and vortexing was preferred to sonication to dissolve KI. KI solution was added to the samples of nanomaterials as received after dispersion (50mg/L), to obtain a typically 1 mL volume sample, with 0.1M KI. 6 x 3 samples were prepared for each nanomaterial/media combination. Additionally, 6 x 3 samples containing 0.1 M KI only and 50mg/L Anatase (Anatase Nanomaterial, Sigma) for each media were prepared as negative and positive controls respectively; 6 nanomaterial samples plus the appropriate controls were prepared and assessed in total. All samples were contained in individual 2mL microcentrifuge tubes. Samples were irradiated under a 1kW Solar Simulator (Newport Corporation, Stratford, CT). The instrument possesses a Personal wavelength correction^{TM} Certificate by Newport. The irradiance of the Solar Simulator was measured to be 1000 Wm^{-2} using an optical power/energy meter (Newport, model 842-PE). Irradiation was performed on groups of 40 microcentrifuge tubes. The tubes were placed vertically under the centre of the lamp of the solar simulator, on an in-house made polystyrene holder, their cups having been removed. The samples were subjected to 10 min periods of irradiation, followed by 5 min period of non-irradiation to reduce sample overheating. After each 10 min period, 1x3 samples for each nanomaterial/media combination and controls were removed from the irradiations. Samples irradiated for 0 min, 10 min, 20 min, 30 min, 40 min and 60 min were collected for each nanomaterial/media combination and corresponding controls. The samples containing nanomaterials were centrifuged at 20800 rcf for 15 min and 800 μL of supernatant was collected in a new micro-centrifuge tube and then analysed using UV-visible spectroscopy (see protocol below).
UV-visible spectroscopy for KI test	The UV-visible spectrum (absorbance scans from 300 nm to 500 nm) was acquired for samples that were irradiated for 60 minutes. Optical absorbance at 352 nm was acquired for all samples. Absorption spectra were acquired with a Lambda 850 UV-Vis spectrometer supported by UV Winlab software [Version 5.1.5] (Perkin Elmer, Waltham, MA). The instrument wavelength calibration was checked using Holmium glass standards (Serial # 9393, Starna Scientific, Hainault, UK). For the reference channel of the spectrophotometer, a matched cell containing the corresponding dispersing media (with no nanoparticles) was used. Absorption spectra were acquired on samples that have been irradiated for 60 minutes. Absorbance scans from 300 nm to 500 nm were performed, using a slit width of 2 nm and a scan rate of 50 nm/min. After each sample, the cuvette was cleaned with a 2% solution of Hellmanex detergent, rinsed with pure water and ethanol and then blow-dried. Optical absorbance at 352 nm was performed using a plate-reader Victor^3 1420 multilabel counter (Perkin Elmer), supported by Wallac 1420 software (Perkin Elmer). 300 μL of each sample (supernatant after centrifugation) was placed in the wells of a 96-well plate. Only the wells of rows 2 to 6 and columns 1 to 10 were used, as they had the same level of noise. The absorption at 352 nm was measured using a 0.1s measurement time. Measured absorption values were displayed on a 0 a.u. to 2 a.u. scale.

Pour (and tapped density measurements), outsourced to Escubed, Leeds	The pour density (sometimes referred to as bulk density) was calculated by measuring a known weight of the solid material, and placing it in a glass measuring cylinder to obtain the volume. In order to measure its tapped density, the cylinder was then tapped mechanically (using a Copley JV2000) by raising and lowering by a set distance until a consistent volume was reached. The volume was measured in order to determine the tapped density; this corresponds to the maximum packing density of the material.
Drum test for dustiness, outsourced to HSL, Buxton, UK	For the EN 15051 standard dustiness measurement, the test apparatus comprised of a 300 mm diameter stainless steel drum (earthed) rotating at 4 rpm, equipped with eight longitudinal vanes to *lift and let fall* a 35 ml volume of the material under test. To determine the mass fractions, the emitted dust cloud was drawn by a vacuum pump at a flow rate of 38 L/min^{-1} for the duration of 1 min (plus a 5 second start up time) through a three-stage porous foam and filter sampling system. Three repeat runs were carried out. Each powder test sample was placed into a 35 ml metal container and weighed; the container was re-weighed after the dust was transferred into the bottom of the drum to work out the mass of sample transferred. The weighed amount was used to calculate the three biologically relevant mass fractions by weighing the weight increase in the porous foams and the glass fibre filter before and after each test. All foams and filters were conditioned overnight inside a humidity and temperature controlled weighing room. An accredited check weight and at least three control foams and filters were weighed alongside each set of samples to adjust for weight changes due to environmental conditions. Also each foam and filter was weighed three times and an average value calculated to ensure that an accurate and precise weight difference was measured. The inhalable fraction was calculated from the increase in weight of the 20 and 80 ppi foams and filter (mg) divided by the amount of powder in the drum (kg). The thoracic fraction is the increased weight of the 80 ppi foam and filter divided by the amount of powder in the drum and the respirable fraction by the increase in weight of the GFA filter/the amount of powder in the drum. All results for the dustiness index were given in terms of the collected weight (mg) in the foams/on the filter divided by the amount of dust in the drum (kg). As dustiness is a function of humidity and temperature, it was also important that environmental conditions were standardized. For all the tests the relative humidity of air entering the drum is maintained at 50% (±10%) and temperatures are at 22 ºC (±2 °C). All powders were tested as supplied but the moisture content was measured using a halogen moisture analyser (Metler Todelo HB43-5) where the dust was dried at about 110 °C and the difference in weight before and after drying measured. The dust was conditioned prior to each run, by passing humidified filtered air through the drum for up to 60 minutes without any rotation, with the dust spread out along the bottom of the drum. The moisture content given in the report is the moisture content of the powder as received before being conditioned in the drum.